MASTER SCIENCES DE LA MATIÈRE
ÉCOLE NORMALE SUPÉRIEURE DE LYON - UNIVERSITÉ CLAUDE BERNARD

Stage de Recherche - Master 2 Physique

Rôle du temps en mécanique quantique
Transition classique-quantique

Vincent Debierre
Stage encadré par **Thomas Durt**
Co-encadrants: **André Nicolet** - **Frédéric Zolla**
Equipe CLARTE

Résumé: L'objet de ce stage était l'étude des systèmes quantiques ouverts et notamment de la décroissance temporelle de leurs états instables. Nous nous sommes intéressés tout d'abord au modèle de Gamow de la désintégration radioactive α, et nous avons confirmé par une étude numérique des résultats analytiques récents concernant les modes propres "à fuites" d'un profil de potentiel inspiré de celui proposé par Gamow. Nous avons ainsi apporté des précisions sur la validité des résultats que permet d'obtenir l'image semi-classique standard d'une particule α rebondissant à l'intérieur d'un puits de potentiel fini. Par la suite nous nous sommes tournés vers l'électrodynamique (quantique) en cavité. À l'aide d'un modèle simple basé sur le couplage de la cavité aux modes de l'extérieur, proche du modèle de Gamow, nous avons étudié la décohérence des états de la cavité, et proposé une démonstration alternative du caractère quasi-classique des états cohérents.

Mots clefs: *Modèle de Gamow - Décroissance temporelle - Électrodynamique en cavité - Décohérence*

Contacts:
`thomas.durt@fresnel.fr` / tél. (+33) 4 91 28 83 28
`andre.nicolet@fresnel.fr` / tél. (+33) 4 91 28 87 73
`frederic.zolla@fresnel.fr` / tél. (+33) 4 91 28 87 79

Institut Fresnel
Campus Universitaire de Saint-Jérôme
Avenue Escadrille Normandie-Niemen
13397 Marseille Cedex

`http://www.fresnel.fr/spip/`

This page intentionally left blank

Remerciements

Je remercie en premier lieu mes trois encadrants qui ont tous, et chacun à sa manière, décuplé mon intérêt et ma motivation pour ce sujet déjà *a priori* attirant. Thomas Durt a su utiliser mes connaissances en mécanique quantique pour me faire voir plus loin que “Shut up and calculate”. Il m’a permis de prendre confiance en moi en mettant en valeur mes résultats. André Nicolet, dont j’ai suivi les cours au niveau de la Licence, a confirmé ce que je savais déjà, à savoir qu’il est un pédagogue passionné et passionnant. Frédéric Zolla s’est quant à lui beaucoup plus impliqué que ce que ne l’exigeait son rôle autoproclamé de “troisième homme”. Je les remercie tous trois chaleureusement, et je suis heureux de pouvoir poursuivre la collaboration en thèse pendant laquelle je pourrai bénéficier de leurs excellents conseils, de leur expertise et de leur humour.

Je remercie également les autres membres de l’équipe CLARTE à l’Institut Fresnel, en particulier Guillaume Demésy, qui m’a initié à l’utilisation de la machine de calcul, Brian Stout, avec qui nous avons eu quelques discussions très intéressantes sur l’électrodynamique classique et quantique, et qui a eu la gentillesse de m’accorder un “prêt longue durée” sur son exemplaire de l’excellent ouvrage *Scattering Theory of Waves and Particles* écrit par R.G. Newton, sans lequel j’aurais été incapable de “rentrer” dans certains calculs, et Gilles Renversez, responsable de l’équipe, qui pour m’avoir enseigné le calcul numérique en C en troisième année de Licence, est condamné pour l’éternité à répondre à mes questions relevant de ce domaine. Je remercie également Nicolas Bonod, le co-responsable de l’équipe, pour son accueil et sa gentillesse.

Je remercie très vivement Benjamin Vial, doctorant de l’équipe MAP2, qui m’a fourni le programme pour l’algorithme de tétrachotomie qu’il a soigneusement développé sous la supervision d’André Nicolet et Frédéric Zolla, et qui m’a apporté son aide à de nombreuses reprises quant à son utilisation.

Je remercie également Frédéric Forestier du service informatique pour son aide, et l’Institut Fresnel dans sa globalité pour son accueil pendant ce stage.

“Prediction is very difficult, especially about the future”, attributed to **Niels Bohr**.

Contents

1 Introduction

Our main interest for this work was the behaviour of quantum unstable states. In a nutshell, we focused on the evolution of initially confined states as they decay with time. Two main topics, along with their well-known respective models, provide the framework and the motivation for our investigations.
The first one is the study of radioactive nuclear decay, especially α decay, for which George Gamow proposed a model [15][16][17] in the late nineteen-twenties. Gamow's work was groundbreaking in the sense that he was the first to make use of the then-brand new quantum theory to study radioactive decay. Though approximate, his model yielded predictions reasonably close to experimental results, which constituted an important success for quantum theory.
The second is the study of cavity quantum electrodynamics (QED) [18], for example experiments carried out by Serge Haroche and his team at the École Normale Supérieure in Paris [19]. In these experiments, light quanta (photons) in the cavity interact with atoms that are injected in order to measure the state of light. The high quality superconducting mirrors which span the inside of the cavity allow for the photons to survive for 130 milliseconds [19] -a spectacular life span- before they are absorbed by the cavity walls. This in turn allows experimentalists to accurately -and repeatedly- measure the number of photons that are present inside the cavity. One can thus monitor the time decay of the photon number.

This document is organised as follows. First we deal with the Gamow model of nuclear decay. We discuss how this model can be refined and how it should be understood, in the light of analytical and numerical results. Thereafter we turn to cavity quantum electrodynamics for which we propose a toy-model inspired by the Gamow model. Using elementary quantum mechanics, we derive the Linblad master equation which is extensively used by cavity QED experimentalists [2] (sect. 4.3).

2 On the quantum mechanical decay of unstable states

In this section we discuss the issue of time decay in quantum mechanics. From a phenomenological point of view, exponential time decay is one of the simplest and most-used models in physics, especially in nuclear physics where it is used to model radioactive decay. Such laws are often derived using classical arguments, and turn out to be very reliable in most cases. However, one can oppose the following argument [4] (sect. 19.1): to derive the exponential decay law, one typically considers a system which consists of many identical unstable atoms, *i.e.* atoms that are prone to decay. The key assumption is that the proportion of atoms that decay in a time interval $\mathrm{d}t$ around t -with respect to the total number of remaining atoms at time t- does not depend on t. This can only be true if the properties of the decaying system remain constant with time, *i.e.* if the system is in a bound state. Clearly, bound states are not decaying states, which shows that the usual heuristic derivation is not without flaw and that the law it allows to derive can at best give a very good approximation of the actual time-decay law -which it often does. We discuss in the following various approaches to the issue.

2.1 The Gamow model

Gamow's goal [15][16][17] was to study nuclear disintegrations, namely, α-type disintegrations

$$\underset{\text{Mother nucleus}}{{}^{A}_{Z}X} \quad \rightarrow \quad \underset{\text{Daughter nucleus}}{{}^{A-4}_{Z-2}Y} \quad + \quad \underset{\text{Helium nucleus}}{{}^{4}_{2}\alpha}$$

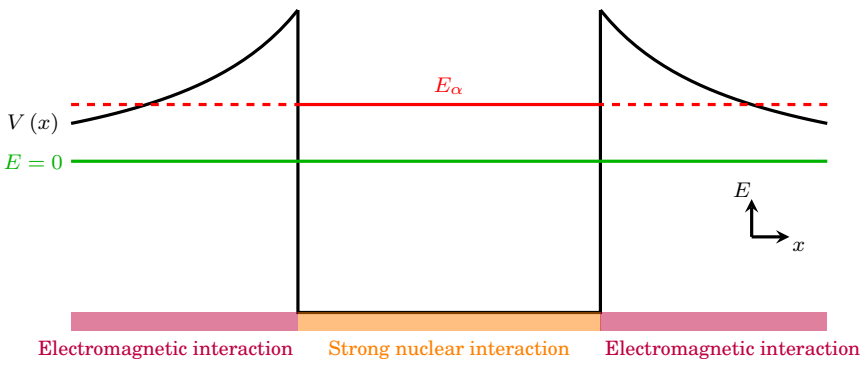

Figure 2.1: Visualisation of the Gamow model. The central zone potential is purely strong force-induced, while it is purely electrostatic outside the strong force range.

within a quantum mechanical framework. To this end, he proposed a simple model: within the mother nucleus, the α particle is a quantum mechanical particle which "sees" the potential created by the other part of the mother nucleus, namely the daughter nucleus. Both strong (nuclear) and electromagnetic (Coulomb) interactions were taken into account by Gamow (he only very grossly modeled the strong force-potential), and the energy E_α of the α particle is assumed to be lower than the barrier height, so that it is in a "quasi-bound" state, but high enough so that it can tunnel through the Coulomb barrier towards the outside world. The situation is schematically represented in Figure 2.1. While we do not discuss the actual Gamow potential in the following, this model laid ground for research on decaying states, which we shall discuss in the following subsections.

2.2 Brief review of analytical results

In this subsection we give some insight on analytical results concerning quantum mechanical scattering problems, focusing on short- and long-time deviations from exponential decay. As far as long-time behaviour is concerned, we typically consider **potentials that vanish outside a region of space**, and here choose the potential to be nonzero in the $[-L, L]$ region only. Using Gamow's idea of complex eigenvalues to the time-independent Schrödinger equation and their associated eigenfunctions, it is possible -though technical- to show that at very long times, the wave function in the $[-L, L]$ region decays as a power law with respect to time (see app. A for details). It is somewhat easier to show [11] that for very short times, the unitarity of the time-evolution operator strictly forbids exponential decay (this is known as the Zeno behaviour). To this end, we focus on the so-called **survival probability** P_{surv} which is defined as the square modulus of the survival amplitude

$$\begin{aligned} A_{\text{surv}}(t) &\equiv \int_{-\infty}^{+\infty} \mathrm{d}x\, \psi^*(x,0)\, \psi(x,t) \\ &= \langle \psi(\cdot,0) \,|\, \mathrm{e}^{-\frac{\mathrm{i}}{\hbar}\hat{H}t}\, \psi(\cdot,0) \rangle. \end{aligned} \tag{2.1}$$

The spectral theorem (see, *e.g.*, [5] (sect. 2)) allows us to rewrite this as an integral over the (in general, continuous and unbounded) spectrum $\sigma(H)$ of $\hat{H}$:

$$\begin{aligned} A_{\text{surv}}(t) &= \int_{\sigma(H)} \mathrm{d}\epsilon\, \langle \psi(\cdot,0) \,|\, \epsilon \rangle \mathrm{e}^{-\frac{\mathrm{i}}{\hbar}\epsilon t} \langle \epsilon \,|\, \psi(\cdot,0) \rangle \\ &= \int_{\sigma(H)} \mathrm{d}\epsilon\, |\langle \psi(\cdot,0) \,|\, \epsilon \rangle|^2\, \mathrm{e}^{-\frac{\mathrm{i}}{\hbar}\epsilon t}. \end{aligned}$$

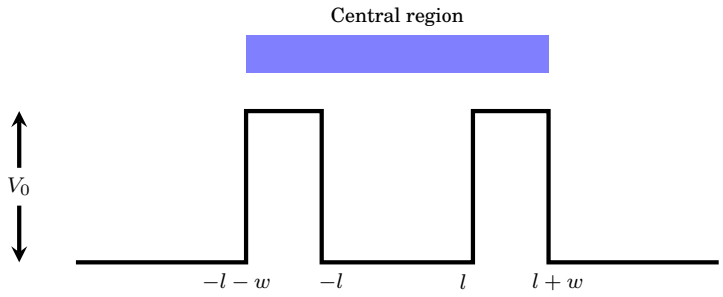

Figure 2.2: The double potential barrier system.

The differentiability of A_{surv} is then guaranteed, using the Lebesgue dominated convergence theorem, by the Cauchy-Schwarz inequality

$$\begin{aligned}\left|\frac{\mathrm{d}A_{\text{surv}}}{\mathrm{d}t}\right| &= \frac{1}{\hbar}\left|\langle\psi(\cdot,0)\,|\,\mathrm{e}^{-\frac{\mathrm{i}}{\hbar}\hat{H}t}\hat{H}\psi(\cdot,0)\rangle\right| \\ &\leq \frac{1}{\hbar}\,||\psi(\cdot,0)||\,||H\psi(\cdot,0)|| \\ &\leq +\infty.\end{aligned}$$

Now, we write:

$$\begin{aligned}P_{\text{surv}}(t) &\equiv |A_{\text{surv}}(t)|^2 \\ &= \left|\langle\psi(\cdot,0)\,|\,\mathrm{e}^{-\frac{\mathrm{i}}{\hbar}\hat{H}t}\,\psi(\cdot,0)\rangle\right|^2 \\ &= \langle\psi(\cdot,0)\,|\,\mathrm{e}^{-\frac{\mathrm{i}}{\hbar}\hat{H}t}\,\psi(\cdot,0)\rangle\left(\langle\psi(\cdot,0)\,|\,\mathrm{e}^{-\frac{\mathrm{i}}{\hbar}\hat{H}t}\,\psi(\cdot,0)\rangle\right)^* \\ &= \langle\psi(\cdot,0)\,|\,\mathrm{e}^{-\frac{\mathrm{i}}{\hbar}\hat{H}t}\,\psi(\cdot,0)\rangle\langle\psi(\cdot,0)\,|\,\mathrm{e}^{\frac{\mathrm{i}}{\hbar}\hat{H}t}\,\psi(\cdot,0)\rangle.\end{aligned}$$

The Cauchy-Schwarz inequality then tells us that $P_{\text{surv}}(t) \leq P_{\text{surv}}(0)$ holds for all t, and, since P_{surv} is differentiable because A_{surv} is, we conclude that $(\mathrm{d}P_{\text{surv}}/\mathrm{d}t)(t=0) = 0$ (since $t=0$ is a maximum of P_{surv}). This shows that the decaying behaviour is non-exponential for small t.

2.3 Numerical simulations: the studied system and the algorithm

The system that we studied is the so-called **double potential barrier**, sketched in Figure 2.2. It features two potential barriers of height V_0 situated between $-l-w$ and $-l$, and l and $l+w$ respectively. We were interested in the decay of a wave packet initially confined between the barriers.

To solve the Schrödinger equation numerically, the easiest path is to treat separately the real part ψ_R and the imaginary part ψ_I of the wave function. This exempts us from manipulating numerically inconvenient (in the framework of the C language) complex quantities. Let Δx be the space discretisation step and Δt the time discretisation step. Following [12], we define the imaginary part and the real part of the wave function to exist at half-step time intervals from each other, in order to use the central difference method to compute the discretised derivatives:

$$\frac{\partial\psi_R}{\partial t}\left(x_m, t_{n+1/2}\right) = \frac{\psi_R\left(x_m, t_{n+1}\right) - \psi_R\left(x_m, t_n\right)}{\Delta t} + \mathrm{o}\left(\Delta t\right), \tag{2.2a}$$

$$\frac{\partial\psi_I}{\partial t}\left(x_m, t_n\right) = \frac{\psi_I\left(x_m, t_{n+1/2}\right) - \psi_I\left(x_m, t_{n-1/2}\right)}{\Delta t} + \mathrm{o}\left(\Delta t\right). \tag{2.2b}$$

Let us now write $\psi^n(m) \equiv \psi(x_m, t_n)$, and define the constants

$$c_1 \equiv \frac{\hbar \Delta t}{2m(\Delta x)^2}, \tag{2.3a}$$

$$c_2 \equiv \frac{\Delta t}{\hbar}. \tag{2.3b}$$

The discretised Schrödinger equation then reads

$$\psi_R^{n+1}(m) = -c_1\left[\psi_I^{n+1/2}(m+1) - 2\psi_I^{n+1/2}(m) + \psi_I^{n+1/2}(m-1)\right] + c_2 V(m)\,\psi_I^{n+1/2}(m) + \psi_R^n(m), \tag{2.4a}$$

$$\psi_I^{n+1/2}(m) = c_1\left[\psi_R^n(m+1) - 2\psi_R^n(m) + \psi_R^n(m-1)\right] - c_2 V(m)\,\psi_R^n(m) + \psi_I^{n-1/2}(m). \tag{2.4b}$$

Useful remarks about the stability of the numerical algorithm can be found in [12]. Before we present some of our results, let us note that this is not the actual equation we solved in our program, since we had to add absorbing layers to avoid reflections. The usual Laplacian operator was thus replaced by a more complicated one. Details are given in app. B which is devoted to the perfectly matched layer (PML) method.

2.4 Overview of results

We discuss here some of the numerical results that we obtained, especially about exponential decay and the difference between two quantities which are often considered in time decay theory: the survival probability and the nonescape probability. Let us mention that our initial state will always be, except when otherwise stated, a Gaußian wave packet

$$\psi(x, t=0) = \left(\pi\sigma^2\right)^{-\frac{1}{4}} \mathrm{e}^{-\frac{x^2}{2\sigma^2}}\,\mathrm{e}^{\mathrm{i}k_0 x} \tag{2.5}$$

where the value of σ is taken so as to confine the initial state between the barriers. The energy E_{free} of such a Gaußian wave packet in free space can be calculated by

$$\begin{aligned}(E_{\text{free}} \equiv)\,\langle\psi(\cdot,t=0)|\,\hat{H}_{\text{free}}\,|\psi(\cdot,t=0)\rangle &= \langle\psi(\cdot,t=0)|\,\frac{\hat{P}^2}{2m}\,|\psi(\cdot,t=0)\rangle \\ &= \frac{1}{2\pi}\int_{-\infty}^{+\infty}\mathrm{d}k\,\frac{\hbar^2k^2}{2m}\left|\bar{\psi}(k,t=0)\right|^2 \\ &= \frac{\hbar^2}{2m}\left(k_0^2 + \frac{1}{\sigma^2}\right).\end{aligned}$$

2.4.1 Short-time behaviour

As expected, we observed a short-time departure from exponential decay when we computed the survival probability against time, as is done in Figure 2.3a where $P_{\text{surv}}(t)$ is plotted at short times for several values of $\alpha \equiv V_0/E_{\text{free}}$ (where V_0, the barrier height, is varied).

2.4.2 Long-time behaviour - The decay constant

The first point we make here is that we always observed exponential decay at long times, regardless of the initial conditions (see Figure 2.4). Unsurprisingly, $\alpha \equiv V_0/E_{\text{free}}$ emerges as a

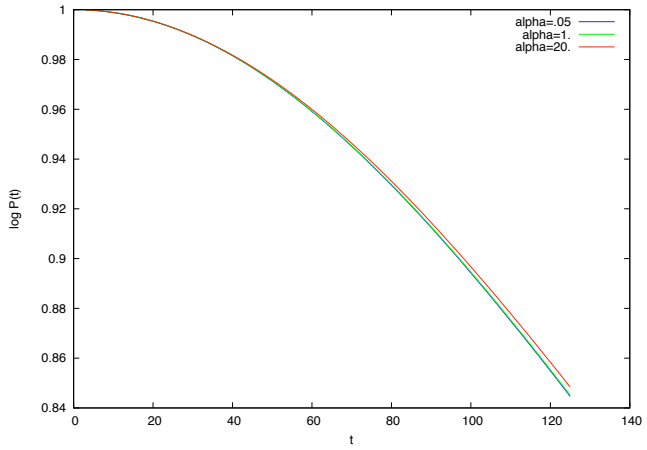

(a) Short-time plots of the survival probability against time for different values of the barrier height V_0. The initial state is the same for all the values of $\alpha = V_0/E_{\text{free}}$ and given by $k_0 = \pi/(2l)$ and $\sigma = (2l)/2.5$ (see (2.5)). As expected, the curve is initially flat and displays a clear departure from exponential decay for short times.

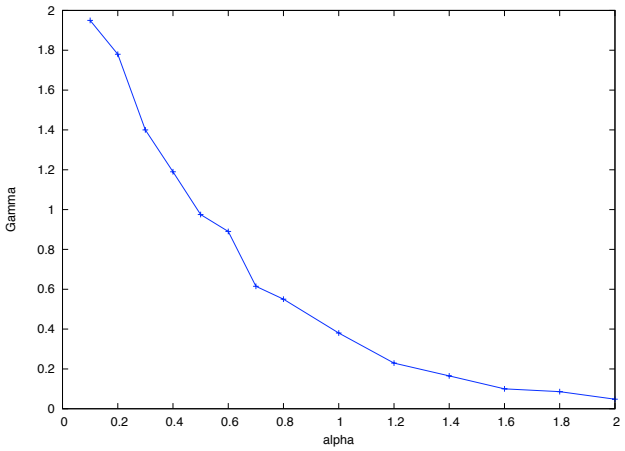

(b) The decay constant Γ in arbitrary units plotted against the reduced barrier height $\alpha = V_0/E_{\text{free}}$ (only V_0 is varied). The initial state is the same for all the values of α and given by $k_0 = \pi/(2l)$ and $\sigma = (2l)/2.5$ (see (2.5)).

Figure 2.3

relevant parameter in the exponential decay, as can be seen in Figure 2.4 where we plotted the logarithm of the nonescape probability

$$P_{\text{nonesc}}(t) \equiv \int_{-l}^{l} \mathrm{d}x \; |\psi(x,t)|^2 \tag{2.6}$$

against time. Defining the decay constant Γ as

$$P_{\text{nonesc}}(t) \underset{t\to+\infty}{\sim} A\,\mathrm{e}^{-\Gamma t} \tag{2.7}$$

one can plot the evolution of Γ with α, as is done in Figure 2.3b.

2.4.3 Survival probability and nonescape probability

While in the present context the most natural quantity to consider in the study of time decay is the nonescape probability (2.6), the survival probability

$$P_{\text{surv}}(t) \equiv \left| \int_{-\infty}^{+\infty} \mathrm{d}x\, \psi^*(x,0)\, \psi(x,t) \right|^2 \tag{2.8}$$

is often considered. The former is the probability to find the particle between the barriers at time t, while the latter measures the wave function's likeness to the initial state. As can be readily verified from the long-time behaviour of the wave function (A.14), the purely exponentially decaying part of both quantities has the same decay constant. This was confirmed numerically (see Figure 2.5b).

2.5 On the "semiclassical" Gamow model

We focus here on the validity of a popular "semiclassical" version of the Gamow model.

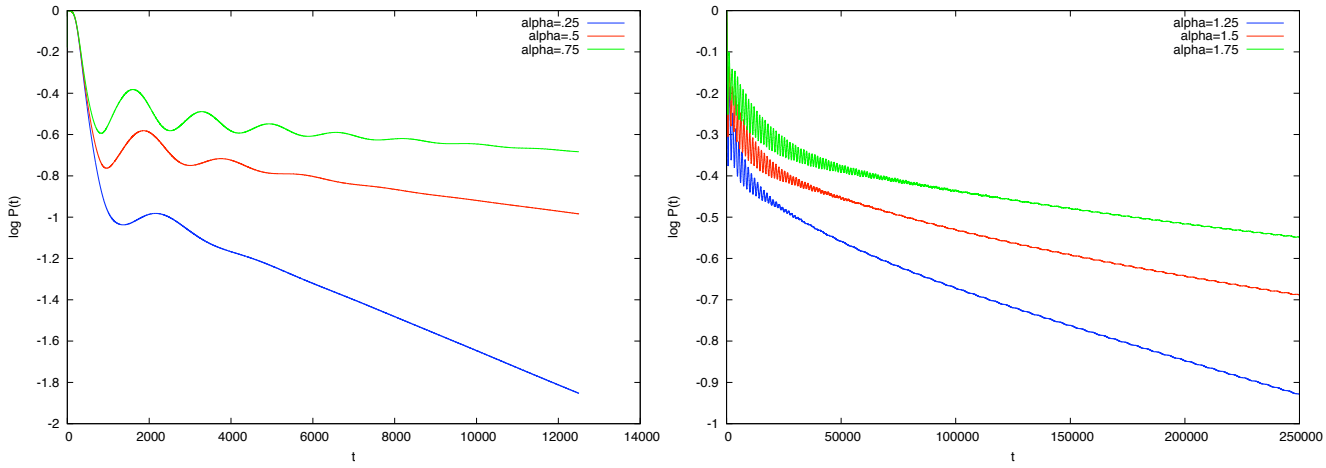

(a) $\alpha < 1$. **(b)** $\alpha > 1$.

Figure 2.4: Plots of the logarithm of the nonescape probability against time for different values of the barrier height V_0: **(a)** $\alpha < 1$ **(b)** $\alpha > 1$. The energy E_{free} of the wave packet is kept constant. The decay is much slower in the latter case. The initial state is the same for all the values of α and given by $k_0 = \pi/(2l)$ and $\sigma = (2l)/5$ (see (2.5)).

2.5.1 The standard "semiclassical" Gamow model

Although it is, unless the author's proficiency in German is even lower than he thinks, not explicitly done is Gamow's original articles [15][16][17], the Gamow model is often [13][14] presented as follows: one takes for granted that the time decay is exponential, and is simply interested in computing the decay constant Γ_G. To this end, one writes it as a product of three factors [14] (we shall call this a "semiclassical" ansatz in the following):

$$\Gamma_G = p(\alpha)\, f\, T \tag{2.9}$$

where

- $p(\alpha)$ is the probability that an α particle exists within the daughter nucleus but is independent from it (it is often taken to be equal to 1 since there is no easy way to evaluate it),
- f is the classical collision frequency between the α particle and the potential barrier created by the daughter nucleus. If one denotes by R_0 the daughter nucleus's radius and v_α the particle's speed, then we can write
$$f = \frac{v_\alpha}{2R_0}, \tag{2.10}$$
- T is the tunneling probability through the potential barrier.

This can be summed up informally in the following way: the α particle oscillates back and forth inside the potential well, every now and then it hits the barrier and a small part of the wave function is transmitted through the barrier. This seems reasonable at first sight, and even at second sight since it allows to derive [14] the empirical Geiger-Nuttal law

$$\log \Gamma_G = \text{cst} - \frac{Z_{\text{daughter}}}{\sqrt{E_\alpha}} \tag{2.11}$$

where E_α is the energy of the α particle and Z_{daughter} is the atomic number of the daughter nucleus. But we shall see that the "semiclassical" ansatz is in fact highly questionable. In particular, the picture of a particle bouncing back and forth provided by (2.10) is at best misleading and eventually dispensable.

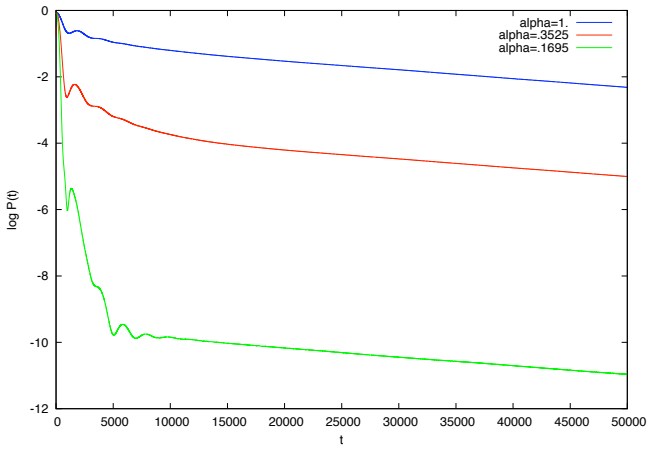

(a) Plots of the logarithm of the nonescape probability against time for different values of the particle's initial energy E_{free}. The barrier height V_0 is kept constant. The initial states are given by $k_0 = \pi/(2l)$ ($\alpha = 1$), $k_0 = 2\pi/(2l)$ ($\alpha = 0.3525$), $k_0 = 3\pi/(2l)$ ($\alpha = 0.1695$), and $\sigma = (2l)/2.5$ for all states (see (2.5)). The initial behaviours are very different but at longer times the exponential decay is identical.

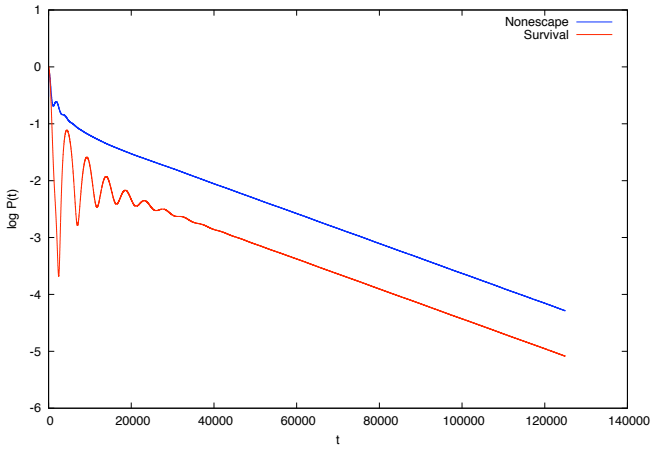

(b) Logarithm of the nonecape probability (2.6) and the survival probability (2.8) plotted against time for $\alpha = 1$. In the exponential regime, the decay constant is the same for both quantities. The initial state is given by $k_0 = \pi/(2l)$ and $\sigma = (2l)/2.5$ (see (2.5)).

Figure 2.5

2.5.2 Refinements and specifications on the model

We start here by presenting rather surprising numerical results which refine our understanding of the Gamow model. Instead of keeping the particle's initial energy E_{free} constant and varying the barrier height V_0 as was done previously, let us keep our potential barrier height constant and vary the initial energy. We plotted in Figure 2.5a the logarithm of the nonescape probability against time, for the same potential barrier height but different initial conditions, *i.e.* different "input" energies. Even though the short-time behaviours are very different, namely, higher energy packets decay much faster at short times, it turns out that at long times, the decay is identical (and exponential) for all initial states. This means that the decay constant is independent of the initial energy, and solely depends on the potential profile which the particle evolves in.

At first sight this seems to be a hard blow dealt at the Gamow model, since we expect the collision frequency, by way of the particle's speed, to depend on the "input" energy (see (2.10)). On the contrary, it appears that the Gamow model remains accurate if we use it wisely, that is, if we focus on the specifications of the state at long times, the wave vector of which can be grossly taken to be equal to $k_{\text{final}} = \pi/(2l)$, as is motivated by the shape of the wave function at long times (see Figure 2.6). Let us for instance consider our system with an initial state given by $k_0 = \pi/(2l)$ and $\alpha = 1$. The particle's mass is taken to be equal to the electron mass $m_e = 9.109 \times 10^{31}$ kg. From the numerical simulations, we obtain the decay rate $\Gamma_{\text{num}} = 1.077 \times 10^{17}\,\text{s}^{-1}$. We can compare this with the results from the "semiclassical" ansatz. Within our algorithm, it is clear that $p(\alpha) = 1$. In order to compute the collision frequency, we make use of the de Broglie identity $\mathbf{p} = \hbar\mathbf{k}$ (with wave vector $k_{\text{final}} = \pi/(2l)$). We use the expression for the intensity transmission coefficient for a square potential barrier [1] (sect. 3.7) to finally obtain $\Gamma_G = 1.868 \times 10^{17}\,\text{s}^{-1}$, which is fairly close to the direct numerical result. Another similar calculation, this time with $\alpha = 5$, gives us a Gamow decay constant of $\Gamma_G = 3.145 \times 10^{14}\,\text{s}^{-1}$ to compare to the direct numerical result $\Gamma_{\text{num}} = 5.511 \times 10^{14}\,\text{s}^{-1}$. Another example is given at the end of app. D.
This shows that, when carefully used, the Gamow model can give a reasonably good approxima-

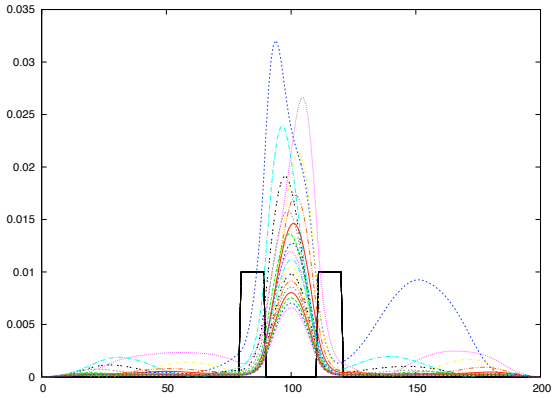

Figure 2.6: Time evolution of the wave function square modulus for $k_0 = \pi/(2l)$ and $\sigma = (2l)/2.5$ (see (2.5)). One sees that Gamow's bouncing picture is valid at short times, but that the wave function rapidly becomes a "quasistationary" wave that leaks through the barriers.

tion of the decay constant. The key step is to forget about the specifications of the initial state, and especially about the "input" energy, and to focus on the final, exponentially decaying state (which is the state the characteristics of which are accessible to the experimentalist who verifies the Geiger-Nuttal law). As a matter of fact, for fixed barrier height, we at first always observed the same final state, *i.e.* the same decay constant. This leads us back to the more formal topic of Gamow functions and complex poles.

2.5.3 Gamow vectors of the problem

Dürr *et al.*'s complex pole approach (see app. D) consists in finding the system's normalised generalised eigenfunctions, which have poles in the complex k-plane. These poles correspond to the system's Gamow functions, *i.e.* solutions of the time-independent Schrödinger equation for complex energy values. More precisely, these complex energy eigenvalues, the imaginary part of which is simply the Gamow function's lifetime, are, up to dimensional factors, the square of the k-values which are the normalised generalised eigenfunctions' poles. These results explain why we always observed the same decay rate for our system when entering "naive" initial states: since the normalised generalised eigenfunctions form a basis -it is indeed their raison d'être- our wave packets were superpositions of Gamow states corresponding to various poles, and only the longest-lived Gamow state survived at long times. Using the tetrachotomy algorithm (see [9] (sect. 3.4) or app. C) to find poles in the complex k-plane, we were able to find other Gamow states and thus to observe other decay constants. This is shown in Figure 2.7a. We see that as announced in [22], the complex pole approach only gives accurate results for long-lived states, that is, for poles associated to eigenenergies with small imaginary part. Subsequent (shorter-lived) Gamow states are less accurately described, that is, they do not necessarily behave differently from the first two Gamow states at long times. In Figure 2.7b we plot the time evolution of the two longest-lived Gamow states. We find that, accordingly to what is inferred in [22], their space-dependence inside and between the barriers is time-invariant and that they simply "melt" with time. These Gamow states can thus be seen as leaky eigenmodes of the system for which the time-dependence can be factored out of a time-independent spatial envelope (see (2.12)). Let us note that they resemble the modes of an infinite potential well (the so-called harmonics), a fact that we shall briefly get back to in the following.

2.5.4 Relevance of the "semiclassical" Gamow model

Since Gamow's picture (or at least the picture which is attributed to him) of a particle that bounces back and forth between the barriers proved rather irrelevant -the "final state" tends to be an (almost) standing wave which leaks through the barriers-, one might wonder why it yields such "accurate" results. In order to explain this, we propose the following argument: at

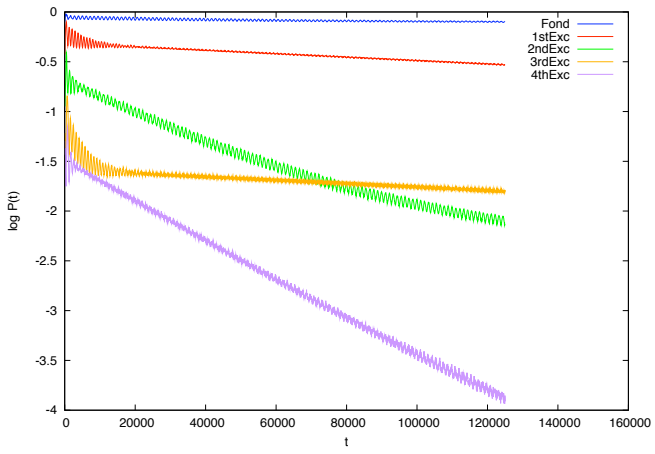

(a) Plots of the logarithm of the nonescape probability against time for the first five Gamow states. The barrier height is kept constant. The initial states are not Gaußian wave packets but the residues of the normalised generalised eigenfunctions (see (D.4)). The results are conclusive for the first two states.

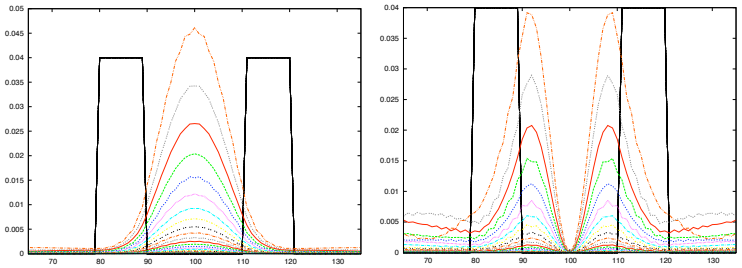

(b) Time evolution of the wave function square modulus for the longest-lived (left) and next-to-longest-lived (right) Gamow states. One sees that the space-dependence of the wave function in the central region (that is, everywhere except in the outside region) is perfectly stationary and that the wave leaks through the barriers.

Figure 2.7

sufficiently long times, and in the central region ($x \in [-l-w, l+w]$), we can write the wave function as

$$\psi(x,t) = \varphi(x)\, \mathrm{e}^{-\frac{\Gamma}{2}t}. \tag{2.12}$$

It is then easily checked that

$$\Gamma = \frac{\frac{\mathrm{d}}{\mathrm{d}t}\int_{-l-w}^{l+w} \mathrm{d}x\ |\psi(x,t)|^2}{\int_{-l-w}^{l+w} \mathrm{d}x\ |\psi(x,t)|^2}.$$

Making use of the probability conservation equation yields

$$\Gamma = \frac{j(l+w,t) - j(-l-w,t)}{\int_{-l-w}^{l+w} \mathrm{d}x\ |\psi(x,t)|^2}$$

where the probability current is given by

$$j(x,t) = \frac{\hbar}{2m\mathrm{i}}\left[\psi^*(x,t)\,\frac{\partial\psi}{\partial x}(x,t) - \psi(x,t)\,\frac{\partial\psi^*}{\partial x}(x,t)\right]. \tag{2.13}$$

The wave function is purely outgoing at the interface between the potential barrier and the outside world, that is, at $x = \pm(l+w)$, which allows us to write

$$\psi(x,t) = A_-\, \mathrm{e}^{-\mathrm{i}kx}\, \mathrm{e}^{-\Gamma t} \quad \text{at } x = -l-w, \tag{2.14a}$$

$$\psi(x,t) = A_+\, \mathrm{e}^{\mathrm{i}kx}\, \mathrm{e}^{-\Gamma t} \quad \text{at } x = l+w \tag{2.14b}$$

and finally yields

$$\Gamma = \frac{\hbar k}{2m(l+w)}\,\frac{|A_+|^2 + |A_-|^2}{\langle|\varphi|^2\rangle_{\text{within}}} \tag{2.15}$$

where $\langle\cdot\rangle_{\text{within}}$ is the average taken over the central region (see Figure 2.2). The first factor in this last equation is of particular interest, since it strongly resembles the bouncing frequency of the "semiclassical" Gamow model (see (2.10)). As for the second factor, it is reminiscent of Gamow's tunneling coefficient, since the latter links the intensity of the wave function at the outer end of the barrier to the intensity of the wave function at its inner end.
Let us mention that in a Bohmian approach, one can get a simple picture of what happens. In

this approach which was first presented by David Bohm in [20], the wave-function is cast in the form

$$\psi(\mathbf{x},t) = R(\mathbf{x},t)\,\mathrm{e}^{\frac{\mathrm{i}}{\hbar}S(\mathbf{x},t)}$$

and the velocity field at x is given by $\mathbf{v}(\mathbf{x},t) = (1/m)\,\nabla S(\mathbf{x},t)$. According to (2.12), one can consider that the velocity vanishes since the space-dependent part is in good approximation real. It is on the other hand obviously nonzero in the outside region, since the wave function propagates outwards.

3 A perturbative treatment for decaying states

We get the following picture from the Bohmian interpretation: either at sufficiently long times for an arbitrary initial state, or at all times for a Gamow state, the particle is trapped inside the barriers without moving, since it must be in a quasi-stationary state $\psi_0(x,t) = \cos(k_{\text{final}}x)\,f(t)$ where $k_{\text{final}} = \pi/(2l)$, and, from time to time, it "jumps" and escapes from the inside region to the the outside region where it moves with velocity[1] $v = \hbar k_{\text{final}}/m$.
Quantum jumps are a major topic among the foundational and interpretational problems of quantum theory. Schrödinger notoriously declared "If we have to go on with these damned quantum jumps, then I'm sorry that I ever got involved". The main problem regarding quantum jumps is that -like other collapse processes- they seemingly violate the quantum mechanical unitarity. In this section we develop a model to describe quantum jumps in a fully unitary formalism. To this end, we introduce an interaction potential which couples the $_{\text{in}}$ and $_{\text{out}}$ states. The price to pay for such a simple, unitary treatment, is that this potential is intrinsically non-local, since it features an instantaneous jump through the potential barriers. On the other hand we shall see that this approach delivers a fully solvable and tractable formalisation of the tunnel process in which all the complexity attached to the resolution of the Schrödinger equation inside the barrier is swept under the rug.

3.1 A quantum jump operator

Our noticing that the Gamow states resemble the infinite potential well eigenstates motivates a perturbative treatment to the problem. However, the fact that the unperturbed system would feature infinite potential regions is a major obstacle as one cannot easily "perturbate oneself out of infinity". Indeed, it is quickly seen that a perturbative treatment from "initial" potential barriers to "final", smaller ones, is very unstable as it strongly depends on the height difference between the "initial" and "final" barriers. In other words, this method is a dead end. Accordingly, we turn to a different treatment where we couple the inside and outside regions through an interaction Hamiltonian.
We make the approximation that the only relevant mode between the barriers is the one which resembles the longest-lived Gamow state. Between the barriers ($|x| < l$) it is equal to $\psi_{\text{in}}(x,t) = \mathrm{e}^{-\mathrm{i}\omega_0 t}\cos(k_0 x)$ where $k_0 = \pi/(2l)$ and $\hbar\omega_0$ is the (real part of the) energy of the longest-lived Gamow state. It is taken to be equal to zero inside the potential barriers and in the outside region (that is, for all $|x| > l$). For "escaping" wave functions outside the barriers we make the natural choice of the basis which consists of plane waves $\psi_{\text{out}}^{\omega,k}(x,t) = \mathrm{e}^{\mathrm{i}(kx-\omega t)}$, with $k > 0$ when $x > w + l$, and $k < 0$ when $x < -w - l$. These functions are also assumed to be equal to zero between and inside the barriers ($-w - l < x < w + l$). This choice is motivated by our interest in the decay of initially confined states. Let us mention that the dispersion relation

[1] Energy conservation is a general property of tunneling processes, therefore $k_{\text{out}}^2 = k_{\text{in}}^2 = k_{\text{final}}^2$.

is to this point unspecified. For a Gamow particle it is obviously quadratic, but photons could (and will) also be considered. The Hamiltonian operator for the system finally reads

$$\hat{H} = \hat{H}_0^{\text{in}} + \hat{H}_0^{\text{out}} + \hat{V}^{\text{jump}} \tag{3.1}$$

where $\hat{H}_0^{\text{in/out}}$ is a standard free-space quantum Hamiltonian mutiplied by the indicator function for the adequate region. As for the quantum jump operator, it reads

$$\hat{V}^{\text{jump}} \equiv \int_0^{+\infty} \mathrm{d}\omega\,(k) \left[\lambda\left(\omega\,(k)\right) |\,\psi_{\text{out}}^{\omega,k}\rangle\langle\psi_{\text{in}}\,| + \lambda^*\left(\omega\,(k)\right) |\,\psi_{\text{in}}\rangle\langle\psi_{\text{out}}^{\omega,k}\,|\right] \tag{3.2}$$

At this level we do not make any specifications on the coupling function λ, but it will be useful in the following to ask that it be sufficiently regular in the vicinity of ω_0, and also that $|\lambda\left(\omega_0\right)|^2/\hbar^2$ is much smaller than ω_0. As we shall see, the latter condition is typical of the Fermi golden rule regime, which is valid when the decay constant Γ is much smaller than the internal frequency ω_0 of the state. We shall also see that, essentially on energy conservation grounds, $|\lambda\left(\omega_0\right)|^2$ is the important parameter here. We shall also give arguments to justify why, in the context of QED cavities, $|\lambda\left(\omega_0\right)|^2$ can be estimated through classical electromagnetic techniques. Finally let us note that our model belongs to the class of the so-called Friedrichs models [25] in which a finite number (N) of discrete states is coupled to a continuum of decay products (here $N = 1$). Our main contribution is to give an explicit spacetime dependence for the decay products (see sect. 3.5), which is not done in the Friedrichs formalism.

3.2 Direct sum and tensor product

The natural structure of the system's Hilbert space $\mathcal{H}$ is given by $\mathcal{H} = \mathcal{H}_{\text{in}} \oplus \mathcal{H}_{\text{out}}$, but here we turn to the different structure of the tensor product (this switch procedure from a direct sum structure to a tensor product structure is detailed in [25]):

$$\mathcal{H} = \mathcal{H}_{\text{in}} \otimes \mathcal{H}_{\text{out}}. \tag{3.3}$$

We can further validate the procedure given in [25] with the following argument: for the direct sum structure one writes a state $|\,\psi^{(i)}\rangle$ as

$$\langle x\,|\,\psi^{(i)}\rangle = \psi_{\text{in}}^{(i)}\,(x)\,\mathbb{1}_{\text{in}}\,(x) + \psi_{\text{out}}^{(i)}\,(x)\,\mathbb{1}_{\text{out}}\,(x) \tag{3.4}$$

where $\mathbb{1}_{\text{in}}$ and $\mathbb{1}_{\text{out}}$ are indicator functions for the in and out regions respectively. Thus the scalar product is given by

$$\langle\psi^{(1)}\,|\,\psi^{(2)}\rangle = \langle\psi_{\text{in}}^{(1)}\mathbb{1}_{\text{in}}\,|\,\psi_{\text{in}}^{(2)}\mathbb{1}_{\text{in}}\rangle + \langle\psi_{\text{out}}^{(1)}\mathbb{1}_{\text{out}}\,|\,\psi_{\text{out}}^{(2)}\mathbb{1}_{\text{out}}\rangle. \tag{3.5}$$

Switching to the tensor product structure, we write

$$|\,\psi^{(i)}\rangle = |\,\psi_{\text{in}}^{(i)}\rangle \otimes |\,0_{\text{out}}\rangle + |\,0_{\text{in}}\rangle \otimes |\,\psi_{\text{out}}^{(i)}\rangle \tag{3.6}$$

where the vacuum states $|\,0_{\text{in/out}}\rangle$ are normalised states. It is then readily found that one gets the same expression as (3.5) for the scalar product. We thus adopt this tensor product structure for the Hilbert space and write the state as follows:

$$|\,\psi\,(t)\rangle = \alpha\,(t)\,|\,1_{\text{in}}\rangle \otimes |\,0_{\text{out}}\rangle + \int \mathrm{d}\omega\,(k)\;\beta\,(k,t)\,|\,0_{\text{in}}\rangle \otimes |\,\omega\,(k)_{\text{out}}\rangle. \tag{3.7}$$

3.3 Time-dependent perturbation theory

We now give some details about the Wigner-Weisskopf approach to perturbation theory. We write the following Hamiltonian for the system:

$$\begin{aligned}\hat{H} =&\hbar\omega_0 \left|1_{\text{in}}\right\rangle\!\left\langle 1_{\text{in}}\right| \otimes \hat{\mathbb{1}}_{\text{out}} + \hat{\mathbb{1}}_{\text{in}} \otimes \int \mathrm{d}\omega\,(k)\ \hbar \left|\omega\,(k)_{\text{out}}\right\rangle\!\left\langle \omega\,(k)_{\text{out}}\right| \\ &+ \int \mathrm{d}\omega\,(k) \left[\lambda\left(\omega\,(k)\right) \left|0_{\text{in}}\right\rangle\!\left\langle 1_{\text{in}}\right| \otimes \left|\omega\,(k)_{\text{out}}\right\rangle\!\left\langle 0_{\text{out}}\right| + \lambda^*\left(\omega\,(k)\right) \left|1_{\text{in}}\right\rangle\!\left\langle 0_{\text{in}}\right| \otimes \left|0_{\text{out}}\right\rangle\!\left\langle \omega\,(k)_{\text{out}}\right|\right].\end{aligned} \tag{3.8}$$

This Hamiltonian is simply the equivalent of the one defined by (3.1) and (3.2) for a tensor product structure. Since the state is initially confined inside the cavity, we choose

$$\begin{cases} \alpha\,(t=0) &= 1, \\ \beta\,(k, t=0) &= 0. \end{cases} \tag{3.9}$$

Noticing that

$$\begin{aligned}\mathrm{i}\hbar\frac{\mathrm{d}\alpha}{\mathrm{d}t} &= \left(\left\langle 1_{\text{in}}\right| \otimes \left\langle 0_{\text{out}}\right|\right) \hat{H} \left|\psi\,(t)\right\rangle, \\ \mathrm{i}\hbar\frac{\partial\beta}{\partial t}\,(k,t) &= \left(\left\langle 0_{\text{in}}\right| \otimes \left\langle \omega\,(k)_{\text{out}}\right|\right) \hat{H} \left|\psi\,(t)\right\rangle\end{aligned}$$

we write coupled equations for the coefficients:

$$\begin{aligned}\mathrm{i}\hbar\frac{\mathrm{d}\alpha}{\mathrm{d}t} &= \hbar\omega_0\alpha\,(t) + \int \mathrm{d}\omega\,(k)\ \lambda^*\left(\omega\,(k)\right)\beta\,(k,t)\,, \\ \mathrm{i}\hbar\frac{\partial\beta}{\partial t}\,(k,t) &= \lambda\left(\omega\,(k)\right)\alpha\,(t) + \hbar\omega\,(k)\,\beta\,(k,t)\,.\end{aligned}$$

Making use of the initial conditions (3.9) yields the following equations [3] (sect. 2.5):

$$\beta\,(k,t) = -\frac{\mathrm{i}}{\hbar}\lambda\left(\omega\,(k)\right)\int_0^t \mathrm{d}t'\,\mathrm{e}^{-\mathrm{i}\omega(k)(t-t')}\alpha\left(t'\right), \tag{3.10a}$$

$$\frac{\mathrm{d}}{\mathrm{d}t}\left(\mathrm{e}^{\mathrm{i}\omega_0 t}\alpha\,(t)\right) = -\int \mathrm{d}\omega\,(k)\left|\frac{\lambda\left(\omega\,(k)\right)}{\hbar}\right|^2 \int_0^t \mathrm{d}t'\,\mathrm{e}^{\mathrm{i}(\omega_0-\omega(k))(t-t')}\left(\mathrm{e}^{\mathrm{i}\omega_0 t'}\alpha\left(t'\right)\right). \tag{3.10b}$$

3.4 Wigner-Weisskopf perturbation theory

We now assume, and it is reasonable, since the self-Hamiltonian of the inside region reads $\hat{H}_{\text{in}} = \hbar\omega_0 \left|1_{\text{in}}\right\rangle\!\left\langle 1_{\text{in}}\right|$, that α is the product of an oscillating exponential of frequency ω_0 with a function f the variations of which are negligible on a time-scale of ω_0^{-1}:

$$\alpha\,(t) = \mathrm{e}^{-\mathrm{i}\omega_0 t} f\,(t)\,. \tag{3.11}$$

One can then write (for a proof of the final step, see, *e.g.*, [26])

$$\begin{aligned}\frac{\mathrm{d}}{\mathrm{d}t}f\,(t) &= -\int \mathrm{d}\omega\,(k)\ \left|\frac{\lambda\left(\omega\,(k)\right)}{\hbar}\right|^2 \int_0^t \mathrm{d}t'\,\mathrm{e}^{\mathrm{i}(\omega_0-\omega(k))(t-t')} f\left(t'\right) \\ &\simeq -\left|\frac{\lambda\left(\omega_0\right)}{\hbar}\right|^2 \int_0^t \mathrm{d}t' \int \mathrm{d}\omega\,(k)\ \mathrm{e}^{\mathrm{i}(\omega_0-\omega(k))(t-t')} f\left(t'\right)\end{aligned}$$

$$= -\left|\frac{\lambda(\omega_0)}{\hbar}\right|^2 \int_0^t \mathrm{d}t'\, 2\pi\, \delta\left(t-t'\right) f\left(t'\right)$$
$$= -\pi\left|\frac{\lambda(\omega_0)}{\hbar}\right|^2 f(t) \tag{3.12}$$

where the second step is approximately valid on energy conservation grounds. This motivates the following Wigner-Weisskopf exponential ansatz (with $\Lambda \equiv \Gamma + 2\mathrm{i}\omega_{\mathrm{LS}}$ a complex-valued number):

$$\alpha(t) = \mathrm{e}^{-\mathrm{i}\omega_0 t}\mathrm{e}^{-\frac{1}{2}\Lambda t}. \tag{3.13}$$

This leads to

$$\frac{1}{2}\Lambda = \mathrm{i}\int \mathrm{d}\omega(k)\left(\frac{\left|\lambda\left(\omega(k)\right)\right|^2}{\hbar^2}\right)\frac{1-\mathrm{e}^{-\mathrm{i}(\omega(k)-\omega_0)t}\mathrm{e}^{\frac{1}{2}\Lambda t}}{\omega_0-\omega(k)-\frac{\mathrm{i}}{2}\Lambda}$$

The Sochocki-Plemelj theorem [7] (sect. 8.1) allows to write, defining the transition rate

$$\Gamma \equiv 2\pi\frac{\left|\lambda(\omega_0)\right|^2}{\hbar^2} \tag{3.14}$$

as well as the Lamb shift

$$\omega_{\mathrm{LS}} \equiv -\frac{1}{\hbar^2}\,\mathrm{vp}\int \mathrm{d}\omega(k)\,\frac{\left|\lambda\left(\omega(k)\right)\right|^2}{\omega(k)-\omega_0}, \tag{3.15}$$

where vp denotes the Cauchy principal value of the subsequent integral, the following expressions [3] (sect. 3.5) for α (compare with (3.12)) and $\beta(k,\cdot)$:

$$\alpha(t) = \mathrm{e}^{-\mathrm{i}(\omega_0+\omega_{\mathrm{LS}})}\mathrm{e}^{-\frac{1}{2}\Gamma t}, \tag{3.16a}$$

$$\beta(k,t) = \mathrm{e}^{-\mathrm{i}\omega(k)t}\frac{\lambda\left(\omega(k)\right)}{\hbar}\frac{1-\mathrm{e}^{-\mathrm{i}(\omega_0+\omega_{\mathrm{LS}}-\omega(k))t}\mathrm{e}^{-\frac{1}{2}\Gamma t}}{\omega(k)-(\omega_0+\omega_{\mathrm{LS}})+\frac{\mathrm{i}}{2}\Gamma}. \tag{3.16b}$$

3.5 Wavefront propagation

Up to this point we focused on massive particles in the non-relativistic regime, but it is straightforward to treat relativistic massless particles with our model (in the following we focus on bosonic particles, and thus take a further step towards cavity quantum electrodynamics). We want to derive an expression for the spacetime dependence of outgoing wave packets in the Wigner-Weisskopf regime. For massless particles these wave packets obey a linear dispersion relation $\omega(x) = ck$, although we note that, in the present regime -that is, the Fermi golden rule regime (see below)- the dispersion relation is in good approximation linear for massive particles as well -with the de Broglie group velocity $v_{\mathrm{dB}} = \hbar k_0/m$ replacing c. This is so because for massive particles $\omega = \hbar k^2/(2m) = \hbar\left(k_0+\delta k\right)^2/(2m)$, and since in the Fermi golden rule regime $\omega_0 >> \delta\omega \approx \Gamma$, we have $\delta k << k_0$ so that $\delta\omega \equiv \omega - \omega_0 \simeq v_{\mathrm{dB}}\delta k$.

In order to make the expressions we are going to manipulate slightly less heavy, we define $\bar{\omega}_0 \equiv \omega_0 + \omega_{\mathrm{LS}}$. We shall now derive the expression for the "photonic wave function" in the outside region. To this end, we shall consider that the wave function is purely outgoing in these regions, which means that we can write

$$\psi_{\mathrm{right}}(x,t) = \mathbb{1}_{\mathrm{right}}(x)\,\frac{1}{\sqrt{2\pi}}\int_{-\infty}^{+\infty}\mathrm{d}k\,\beta(k,t)\,\mathrm{e}^{\mathrm{i}kx}, \tag{3.17a}$$

$$\psi_{\mathrm{left}}(x,t) = \mathbb{1}_{\mathrm{left}}(x)\,\frac{1}{\sqrt{2\pi}}\int_{-\infty}^{+\infty}\mathrm{d}k\,\beta(k,t)\,\mathrm{e}^{-\mathrm{i}kx} \tag{3.17b}$$

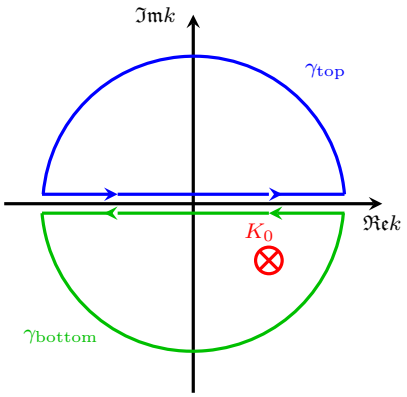

Figure 3.1: Jordan loops in the complex k-plane used to compute the integrals (3.18). The (isolated) simple pole $K_0 = (1/c)\left[\bar{\omega}_0 - \mathrm{i}\left(\pi/\hbar^2\right)|\lambda(\omega_0)|^2\right]$ of the integrands is represented by the red circled cross.

where $\mathbb{1}_{\mathrm{right}}$ and $\mathbb{1}_{\mathrm{left}}$ are indicator functions for the right and left regions respectively. From the expression of β (see (3.16)) we get

$$\psi_{\mathrm{right}}(x,t) = \mathbb{1}_{\mathrm{right}}(x)\frac{1}{\sqrt{2\pi}}\int_{-\infty}^{+\infty}\mathrm{d}k\,\frac{\lambda(ck)}{ck-\bar{\omega}_0+\mathrm{i}\frac{\pi}{\hbar^2}|\lambda(\omega_0)|^2}\left[\mathrm{e}^{\mathrm{i}k(x-ct)} - \mathrm{e}^{-\mathrm{i}(\bar{\omega}_0 t - kx)}\mathrm{e}^{-\frac{\pi}{\hbar^2}|\lambda(\omega_0)|^2 t}\right] \tag{3.18a}$$

$$\equiv \mathbb{1}_{\mathrm{right}}(x)\frac{1}{\sqrt{2\pi}}\left[I_{\mathrm{right}}(x-ct) - J_{\mathrm{right}}(x)\right],$$

$$\psi_{\mathrm{left}}(x,t) = \mathbb{1}_{\mathrm{left}}(x)\frac{1}{\sqrt{2\pi}}\int_{-\infty}^{+\infty}\mathrm{d}k\,\frac{\lambda(ck)}{ck-\bar{\omega}_0+\mathrm{i}\frac{\pi}{\hbar^2}|\lambda(\omega_0)|^2}\left[\mathrm{e}^{-\mathrm{i}k(x+ct)} - \mathrm{e}^{-\mathrm{i}(\bar{\omega}_0 t + kx)}\mathrm{e}^{-\frac{\pi}{\hbar^2}|\lambda(\omega_0)|^2 t}\right] \tag{3.18b}$$

$$\equiv \mathbb{1}_{\mathrm{left}}(x)\frac{1}{\sqrt{2\pi}}\left[I_{\mathrm{left}}(x+ct) - J_{\mathrm{left}}(x)\right].$$

To compute these integrals, we use the Cauchy residue theorem along the Jordan loops drawn on Figure 3.1. We see that the pole K_0 of the integrands is always

$$K_0 = \frac{1}{c}\left[\bar{\omega}_0 - \mathrm{i}\frac{\pi}{\hbar^2}|\lambda(\omega_0)|^2\right] \tag{3.19}$$

Let us first deal with the Js. We are only interested in $J_{\mathrm{right}}(x)$ when $\mathbb{1}_{\mathrm{right}}(x)$ does not vanish, that is, when $x > 0$. In this case, one uses the Jordan loop γ_{top} and one sees that $J_{\mathrm{right}}(x) = 0$, which means that this integral never contributes to (3.18a). With a similar reasoning, we see that $J_{\mathrm{left}}(x)$ does not contribute to (3.18b). We now turn to the Is, and focus on I_{right}. For $x - ct > 0$, We use the Jordan loop γ_{top}, and thus $I_{\mathrm{right}}(x-ct)$ vanishes. For $x - ct = 0$, we immediately see that the integral diverges. For $x - ct < 0$, we use the Jordan loop γ_{bottom} which yields $I_{\mathrm{right}}(x-ct) = -2\mathrm{i}\pi\,\lambda(\bar{\omega}_0)\,\mathrm{e}^{\frac{\mathrm{i}}{c}\left(\bar{\omega}_0 - \mathrm{i}\frac{\pi}{\hbar^2}|\lambda(\omega_0)|^2\right)(x-ct)}$ (where the value of λ is taken at $\bar{\omega}_0$ since this function has meaning for real values of the argument only). A similar reasoning is valid for I_{left} and we finally get

$$\psi_{\mathrm{right}}(x,t) = \mathbb{1}_{\mathrm{right}}(x)\,\Theta(ct-x)\frac{\lambda(\bar{\omega}_0)}{\sqrt{2\pi}}(-2\mathrm{i}\pi)\,\mathrm{e}^{\frac{\mathrm{i}}{c}\left(\bar{\omega}_0 - \mathrm{i}\frac{\pi}{\hbar^2}|\lambda(\omega_0)|^2\right)(x-ct)}, \tag{3.20a}$$

$$\psi_{\mathrm{left}}(x,t) = \mathbb{1}_{\mathrm{left}}(x)\,\Theta(ct+x)\frac{\lambda(\bar{\omega}_0)}{\sqrt{2\pi}}(-2\mathrm{i}\pi)\,\mathrm{e}^{\frac{\mathrm{i}}{c}\left(\bar{\omega}_0 - \mathrm{i}\frac{\pi}{\hbar^2}|\lambda(\omega_0)|^2\right)(x+ct)}. \tag{3.20b}$$

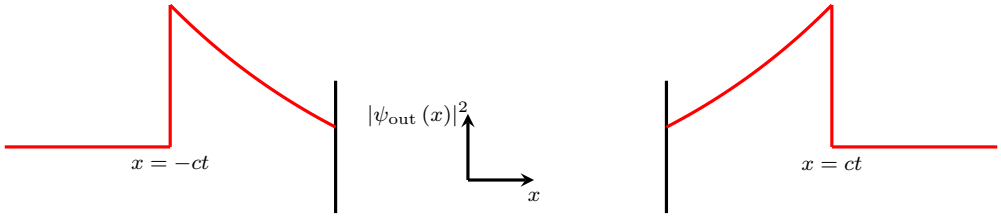

Figure 3.2: Profile of the wave function square modulus in the outside region at fixed time. It increases exponentially with increasing $\pm x$ (see text and (3.20) and vanishes outside the light cone.

Thus we see that the wave function is nonvanishing inside the light cone only. At fixed time, it increases exponentially with increasing x or $-x$, depending on whether we look at what happens on the right or on the left of the inside region. This is sketched in Figure 3.2. We saw that the wave function is ill-defined on the light cone, but we can continuously extend it from the inside of the light cone to the $x = \pm ct$ points (where there is a discontinuity anyway). The exponential growth is strongly reminiscent of what is obtained in the framework of Gamow functions (for massive particles) [22], as well as in the case of a non-quantum treatment of an open electromagnetic system (see [35] for more details and/or the discussion at the end of sect. 4.2 for a quick and informal presentation of the method which yields this kind of results). It is still an open question whether it is possible to associate a wave function to a photon [36]. This is so because there exists no first quantised version of quantum optics, and the non-relativistic limit of quantum optics is problematic. We do not enter details here but nothing forbids us to consider the right and left outgoing wave packets (3.20) to be good candidates for photonic wave functions. Interestingly, a simple Bohmian picture holds for these outgoing waves. Indeed the outgoing right (resp. left) wave function defined by (3.17) obeys[2] in the right (resp. left) region $\partial\Psi/\partial t = \pm c\,\partial\Psi/\partial x$, so that $j(x,t) = \pm c\,\rho(x,t)$ where $\rho(x,t) = |\psi(x,t)|^2$ and $j(x,t)$ is defined by (2.13). The Bohmian velocity reads $v_{\text{Bohm}}(x,t) \equiv j(x,t)/\rho(x,t) = \pm c$, and thus we recover the old Einsteinian picture of a photon moving at the speed of light in the outside region. Between the barriers, however, the particles are at rest in the Bohmian picture, regardless of their mass.

4 Decoherence in cavity quantum electrodynamics

In this section we present a simple approach to the study of decoherence in a QED cavity. We study the behaviour of the cavity's coherent states and use our results to address the quantum-classical limit, notably in the light of the so-called quantum darwinist approach. In cavity QED experiments, photons are kept in a "box" (superconducting cavity) during "macroscopic" times (130 milliseconds at the time of [19]), after which they are absorbed by the cavity walls. This picture is reminiscent of the decay of α particles confined in a potential well. We propose the following model for photon emission in cavity QED experiments. The Maxwell field inside the cavity has states $|\,0_{\text{in}}\rangle$ and $|\,1_{\text{in}}\rangle$, and it is coupled to the "outside world" which possesses a continuous infinity of modes (see Figure 4.1). This model is perfectly identical to the one defined in sect. 3, so that the results derived within the framework of the Wigner-Weisskopf approach are immediately relevant here. We make use of these results to study decoherence in QED cavities.

[2]This is also true in the case of massive particles, but then c should be replaced by the de Broglie velocity $v_{\text{dB}} = \hbar k_0/m$.

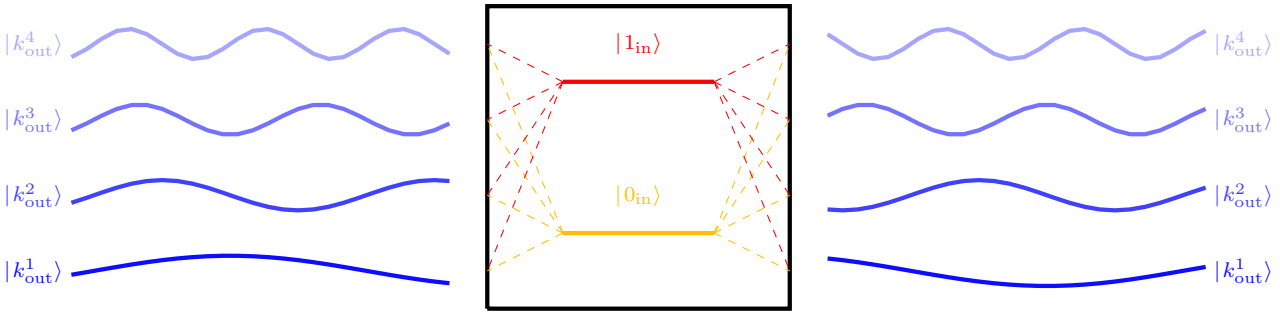

Figure 4.1: Toy-model for cavity QED. A two-state field inside the box is coupled to the continuum of free space modes that exists outside.

4.1 Decoherence and pointer states

Before entering the specific details of the system, we present the basic features of the decoherence program.

4.1.1 Motivations and goals of the decoherence program

Although its building blocks are quantum and thus obey the famous superposition principle -a linear combination of solutions to the Schrödinger equation constitutes another -perfectly valid- solution to the Schrödinger equation- the macroscopic world clearly displays a departure from such superpositions. The decoherence program is aimed at explaining why the macroscopic world does not (directly) obey quantum mechanical laws. It is based on the insight that quantum systems are never isolated [32], but that their evolution is at least partly monitored by their environment with which it continuously interacts (as is put in [2] (sect. 4), "the environment is watching"). The decoherence program's goal is to build on this insight to explain how the "classical" properties of the macroscopic world can be retrieved from a purely quantum mechanical paradigm at the micropscopic level. In this approach, one can show [27] [29] how the interaction between the system and its environment destroys the coherence between a paticular set of quantum states, the so-called "pointer states", which correspond to the "pointer" positions of the macroscopic measurement apparatus, *i.e.*, the different outcomes of a macroscopic measurement performed on the system [32].

4.1.2 Pointer states and quantum darwinism

As is indicated by the fact that they are associated to the outcomes of macroscopic measurements on a system, the so-called quantum pointer states are "quasi-classical" states of a quantum system. In a nutshell, they are singled out by their robustness to the interaction between the system and its environment, which explains why considerations on pointer states are referred to as "quantum darwinism". To give the "robustness" criterion a mathematical significance, we turn to the decoherence theorist's favourite tool, the reduced density matrix

$$\hat{\rho}_S(t) \equiv \text{Tr}_E\left(|\psi(t)\rangle\langle\psi(t)|\right) \tag{4.1}$$

where $|\psi(t)\rangle$ is simply the state of the full system -that is, the system and its environment- at time t and the partial trace is taken over the environment's degrees of freedom. Pointer states are then defined as the states which minimise the system's information loss, that is, they minimise the system's Shannon-von Neumann entropy [30]

$$S(t) \equiv -\text{Tr}_S\left[\hat{\rho}_S(t)\log\left(\hat{\rho}_S(t)\right)\right]. \tag{4.2}$$

It is well-known that, since decoherence is the corollary of entanglement [24], pointer states of the system can be defined as the states which become minimally entangled with the environment in the course of their evolution [31]. In our model, the inside region plays the part of the system while the outside region is the environment.

4.2 On the evolution of coherent states

Let us write symbolically

$$|1_{\text{out}}\rangle \equiv \int \mathrm{d}\omega\,(k)\ \beta\,(k,t))\ |\omega\,(k)_{\text{out}}\rangle. \tag{4.3}$$

We know from sect. 3 that an initially confined state $|1_{\text{in}}\rangle\otimes|0_{\text{out}}\rangle$ evolves into $\alpha\,(t)\ |1_{\text{in}}\rangle\otimes|0_{\text{out}}\rangle+\beta\,(t)\ |0_{\text{in}}\rangle\otimes|1_{\text{out}}\rangle$. Thus, we can write the following time-evolution for n (undistinguishable) bosons which we label with the index k:

$$\begin{aligned}\bigotimes_{k=1}^{n}\left(|1_{\text{in}}\rangle_k\otimes|0_{\text{out}}\rangle_k\right) &\xrightarrow{t} \bigotimes_{k=1}^{n}\left(\alpha\,(t)\ |1_{\text{in}}\rangle_k\otimes|0_{\text{out}}\rangle_k+\beta\,(t)\ |0_{\text{in}}\rangle_k\otimes|1_{\text{out}}\rangle_k\right)\\ &=\sum_{j=0}^{n}\alpha^j\,(t)\,\beta^{n-j}\,(t)\sqrt{\frac{n!}{j!\,(n-j)!}}\ |j_{\text{in}}\rangle\otimes|\,(n-j)_{\text{out}}\rangle.\end{aligned} \tag{4.4}$$

This result can be proved thusly: the normalised states $|\,j_{\text{in}}\rangle\otimes|\,(n-j)_{\text{out}}\rangle$ are defined by symmetrization over all possible states having j particles in and $(n-j)$ particles out. The corresponding nonnormalised states read

$$\underbrace{\left[|\,j_{\text{in}}\rangle\otimes|\,(n-j)_{\text{out}}\rangle\right]_{\text{non}}}_{\text{all other combinations with } j \text{ in}} \equiv \underbrace{\left(\left(|\,1_{\text{in}}\rangle_1\otimes|0_{\text{out}}\rangle_1\right)\otimes\ldots\otimes\left(|\,1_{\text{in}}\rangle_j\otimes|0_{\text{out}}\rangle_j\right)\right)}_{j \text{ times}}\otimes\underbrace{\left(\left(|\,0_{\text{in}}\rangle_{j+1}\otimes|\,1_{\text{out}}\rangle_{j+1}\right)\otimes\ldots\otimes\left(|\,0_{\text{in}}\rangle_n\otimes\ |1_{\text{out}}\rangle_n\right)\right)}_{(n-j) \text{ times}}$$

and $(n-j)$ out.

There are $(n!)\,/\,(j!\,(n-j)!)$ such combinations, which means that

$$|\,j_{\text{in}}\rangle\otimes|\,(n-j)_{\text{out}}\rangle=\sqrt{\frac{j!\,(n-j)!}{n!}}\ \left[|\,j_{\text{in}}\rangle\otimes|\,(n-j)_{\text{out}}\rangle\right]_{\text{non}}. \tag{4.5}$$

It is straightforward to see that

$$\bigotimes_{k=1}^{n}\left(\alpha\,(t)\ |1_{\text{in}}\rangle_k\otimes|0_{\text{out}}\rangle_k+\beta\,(t)\ |0_{\text{in}}\rangle_k\otimes|1_{\text{out}}\rangle_k\right)=\left[|\,j_{\text{in}}\rangle\otimes|\,(n-j)_{\text{out}}\rangle\right]_{\text{non}}$$

which along with (4.5) proves (4.4). In particular, if at time $t=0$ the cavity is prepared in a coherent state and the exterior is in its vacuum state, then the evolution yields coherent states for the exterior:

$$\begin{aligned}|\,\psi\,(t=0)\rangle &= \mathrm{e}^{-\frac{|\xi|^2}{2}}\sum_{n=0}^{+\infty}\frac{\xi^n}{\sqrt{n!}}\ |n_{\text{in}}\rangle\otimes|0_{\text{out}}\rangle\\ \rightarrow|\,\psi\,(t)\rangle &= \mathrm{e}^{-\frac{|\xi|^2}{2}|\alpha(t)|^2}\sum_{n=0}^{+\infty}\sum_{m=0}^{n}\frac{(\xi\alpha\,(t))^m}{\sqrt{m!}}\ |m_{\text{in}}\rangle\otimes\mathrm{e}^{-\frac{|\xi|}{2}|\beta(t)|^2}\frac{(\xi\beta\,(t))^{n-m}}{\sqrt{(n-m)!}}\ |\,(n-m)_{\text{out}}\rangle\end{aligned} \tag{4.6}$$

where we used the identity $|\alpha(t)|^2 + |\beta(t)|^2 = 1$. The state at time t can be rewritten as

$$|\psi(t)\rangle = \mathrm{e}^{-\frac{|\xi|^2}{2}|\alpha(t)|^2} \sum_{k=0}^{+\infty} \frac{(\xi\alpha(t))^k}{\sqrt{k!}} |k_{\mathrm{in}}\rangle \otimes \mathrm{e}^{-\frac{|\xi|^2}{2}|\beta(t)|^2} \sum_{m=0}^{+\infty} \frac{(\xi\beta(t))^m}{\sqrt{m!}} |m_{\mathrm{out}}\rangle. \tag{4.7}$$

This establishes that coherent states of the cavity interact with the exterior without getting entangled with it. They can thus be considered as "classical pointers" according to the criterion for classicality derived by Zurek in the framework of the quantum darwinist approach. Furthermore Schrödinger noted [33] that coherent states are as close as possible to classical systems, *i.e.*, their phase-space fluctuations saturate the Heisenberg uncertainties. Moreover these fluctuations remain the same when the average number $|\xi|^2$ of elementary excitations increases. In the high-energy limit they can thus consistently be neglected.

All these elements indicate that in the limit of high-energy coherent states, it is likely that Maxwell's equations will in good approximation be valid, which somewhat motivates why the dissipation factor Γ of a QED cavity can be taken to be equal to the classical dissipation factor. This is so because the correspondence principle is fully justified in the case of (high-energy) coherent states. This is particularly interesting since André Nicolet and Frédéric Zolla, along with their PhD student Benjamin Vial and others [35], have developed a numercial method to compute the electromagnetic eigenmodes of arbitrary systems. This method is based on the resolution (with the finite-element method) of the source-free Maxwell's equations so as to find the system's eigenmodes (it is, as Frédéric Zolla would put it, "the electromagnetic equivalent of figuring out what a music instrument sounds like without playing it"). The systems considered are open systems, the numerical study of which is made possible by the use of perfectly matched layers which simulate the infinity of space. Complex eigenfrequencies are found, the real part of which is a resonance frequency of the system, while their imaginary parts are the dissipation factors.

4.3 On the Lindblad master equation

The Lindblad master equation is a widely used dissipative (*i.e.* nonunitary) equation which models the coherence loss which a quantum system undergoes when it interacts with its environment. It governs the studied system's reduced density matrix, and, in the case of a QED cavity (at zero temperature), it reads [2] (sect. 7.5.1)

$$\frac{\mathrm{d}}{\mathrm{d}t}\hat{\rho}_{\mathrm{in}}(t) = \frac{1}{\mathrm{i}\hbar}\left[\hat{H}, \hat{\rho}_{\mathrm{in}}(t)\right] + \frac{\Gamma}{2}\left[2\hat{a}\hat{\rho}_{\mathrm{in}}(t)\,\hat{a}^\dagger - \hat{a}^\dagger\hat{a}\hat{\rho}_{\mathrm{in}}(t) - \hat{\rho}_{\mathrm{in}}(t)\,\hat{a}^\dagger\hat{a}\right]. \tag{4.8}$$

4.3.1 The Lindblad master equation and quantum Monte-Carlo trajectories

A common way to derive the Lindblad master equation is to introduce the so-called quantum Monte-Carlo trajectories. These trajectories are built such that the density matrix of the full system (that is, the cavity and its environment) is retrieved when the average over the Monte-Carlo trajectories is taken. This method is simply a convenient way to compute the trace over the environment's degrees of freedom [2] (sect. 7.5.2). For a QED cavity, the derivation can be sketched out as follows: we assume that at time t the cavity is in a n photon-Fock state. During the time interval $[t, t + \mathrm{d}t]$, one elementary excitation of the system is dissipated in the environment with probability $\Gamma n\,\mathrm{d}t$, in which case the cavity state at time t should be replaced by the properly normalised $(n-1)$ photon Fock state at time $t + \mathrm{d}t$. Otherwise (and this happens with probability $(1 - \Gamma n\,\mathrm{d}t)$), no excitation is released, and the state is simply appropriately normalised. The master equation (4.8) is then obtained.

4.3.2 Derivation of the Linblad master equation in terms of damped coherent states

We propose here an alternate derivation of the Lindblad master equation. Our proof is based on the fact that any damped coherent state of the form

$$|\xi_{\text{in}}(t)\rangle = \mathrm{e}^{-\frac{|\xi|^2}{2}|\alpha(t)|^2} \sum_{m=0}^{+\infty} \frac{(\xi\alpha(t))^m}{\sqrt{m!}} |m_{\text{in}}\rangle, \tag{4.9}$$

with α given by (3.16) and $\hat{H} = \hbar\omega\hat{a}^\dagger\hat{a}$, obeys the Lindblad equation (4.8). To prove this first assessment we write the system's reduced density matrix for coherent states of the form (4.7). It is straightforward to see that it reads

$$\hat{\rho}_{\text{in}}(t) = \mathrm{e}^{-|\xi\alpha(t)|^2} \sum_{k=0}^{+\infty}\sum_{n=0}^{+\infty} \frac{(\xi\alpha(t))^k}{\sqrt{k!}} \frac{(\xi^*\alpha^*(t))^n}{\sqrt{n!}} |k_{\text{in}}\rangle\langle n_{\text{in}}|. \tag{4.10}$$

It is clear that the corresponding reduced state is (4.9). Hence, proving that the density matrix (4.10) satisfies the master equation proves that coherent states of the form (4.9) are solutions to the Lindblad master equation. To that end, we proceed to differentiate the reduced density matrix with respect to time:

$$\begin{aligned}
\frac{\mathrm{d}}{\mathrm{d}t}\hat{\rho}_{\text{in}}(t) = \mathrm{e}^{-|\xi\alpha(t)|^2} \Bigg[& -|\xi|^2 \frac{\mathrm{d}}{\mathrm{d}t}|\alpha(t)|^2 \sum_{k=0}^{+\infty}\sum_{n=0}^{+\infty} \frac{(\xi\alpha(t))^k}{\sqrt{k!}} \frac{(\xi^*\alpha^*(t))^n}{\sqrt{n!}} |k_{\text{in}}\rangle\langle n_{\text{in}}| \\
& + \sum_{k=1}^{+\infty}\sum_{n=1}^{+\infty} \left(k\xi\frac{\mathrm{d}\alpha}{\mathrm{d}t}\xi^*\alpha^*(t) + n\xi^*\frac{\mathrm{d}\alpha^*}{\mathrm{d}t}\xi\alpha^*(t) \right) \frac{(\xi\alpha(t))^{k-1}}{\sqrt{k!}} \frac{(\xi^*\alpha^*(t))^{n-1}}{\sqrt{n!}} |k_{\text{in}}\rangle\langle n_{\text{in}}| \Bigg] \\
= \mathrm{e}^{-|\xi\alpha(t)|^2} & \sum_{k=0}^{+\infty}\sum_{n=0}^{+\infty} \left[-|\xi|^2 \frac{\mathrm{d}}{\mathrm{d}t}|\alpha(t)|^2 + \left(\frac{k}{\alpha(t)}\frac{\mathrm{d}\alpha}{\mathrm{d}t} + \frac{n}{\alpha^*(t)}\frac{\mathrm{d}\alpha^*}{\mathrm{d}t} \right) \right] \frac{(\xi\alpha(t))^k}{\sqrt{k!}} \frac{(\xi^*\alpha^*(t))^n}{\sqrt{n!}} |k_{\text{in}}\rangle\langle n_{\text{in}}|.
\end{aligned}$$

We now use the Wigner-Weisskopf expression (3.16) for α:

$$\alpha(t) = \mathrm{e}^{-\mathrm{i}\omega t}\mathrm{e}^{-\frac{1}{2}\Gamma t} \tag{4.11}$$

which yields

$$\frac{\mathrm{d}}{\mathrm{d}t}\hat{\rho}_{\text{in}}(t) = \mathrm{e}^{-|\xi\alpha(t)|^2} \sum_{k=0}^{+\infty}\sum_{n=0}^{+\infty} \left[\Gamma\left(|\xi|^2|\alpha(t)|^2 - \frac{1}{2}(k+n) \right) - \mathrm{i}\omega(k-n) \right] \frac{(\xi\alpha(t))^k}{\sqrt{k!}} \frac{(\xi^*\alpha^*(t))^n}{\sqrt{n!}} |k_{\text{in}}\rangle\langle n_{\text{in}}|.$$

We now compare this to the right-hand side of (4.8) (recalling that $H = \hbar\omega\hat{a}^\dagger\hat{a}$):

$$\begin{aligned}
\frac{1}{\mathrm{i}\hbar}\left[\hat{H}, \hat{\rho}_{\text{in}}(t)\right] &= \frac{1}{\mathrm{i}}\mathrm{e}^{-|\xi\alpha(t)|^2} \sum_{k=0}^{+\infty}\sum_{n=0}^{+\infty} \frac{(\xi\alpha(t))^k}{\sqrt{k!}} \frac{(\xi^*\alpha^*(t))^n}{\sqrt{n!}} \left[\omega\hat{a}^\dagger\hat{a}, |k_{\text{in}}\rangle\langle n_{\text{in}}|\right] \\
&= -\mathrm{i}\,\mathrm{e}^{-|\xi\alpha(t)|^2} \sum_{k=0}^{+\infty}\sum_{n=0}^{+\infty} \frac{(\xi\alpha(t))^k}{\sqrt{k!}} \frac{(\xi^*\alpha^*(t))^n}{\sqrt{n!}} \omega(k-n) |k_{\text{in}}\rangle\langle n_{\text{in}}|,
\end{aligned}$$

while

$$\begin{aligned}
& \frac{\Gamma}{2}\left[2a\hat{\rho}_{\text{in}}(t)\hat{a}^\dagger - \hat{a}^\dagger\hat{a}\hat{\rho}_{\text{in}}(t) - \hat{\rho}_{\text{in}}(t)\hat{a}^\dagger\hat{a}\right] \\
& = \mathrm{e}^{-|\xi\alpha(t)|^2} \left[2\sum_{k=1}^{+\infty}\sum_{n=1}^{+\infty} \frac{(\xi\alpha(t))^k}{\sqrt{k!}} \frac{(\xi^*\alpha^*(t))^n}{\sqrt{n!}} \sqrt{kn}\, |(k-1)_{\text{in}}\rangle\langle(n-1)_{\text{in}}| \right.
\end{aligned}$$

$$
\begin{aligned}
&-\sum_{k=0}^{+\infty}\sum_{n=0}^{+\infty}\left[\frac{\left(\xi\alpha\left(t\right)\right)^{k}}{\sqrt{k!}}\frac{\left(\xi^{*}\alpha^{*}\left(t\right)\right)^{n}}{\sqrt{n!}}k-\frac{\left(\xi\alpha\left(t\right)\right)^{k}}{\sqrt{k!}}\frac{\left(\xi^{*}\alpha^{*}\left(t\right)\right)^{n}}{\sqrt{n!}}n\right]\left|k_{\mathrm{in}}\right\rangle\left\langle n_{\mathrm{in}}\right|\Bigg] \\
&=\mathrm{e}^{-\left|\xi\alpha(t)\right|^{2}}\sum_{k=0}^{+\infty}\sum_{n=0}^{+\infty}\left[2\left|\xi\right|^{2}\left|\alpha\left(t\right)\right|^{2}-\left(k+n\right)\right]\frac{\left(\xi\alpha\left(t\right)\right)^{k}}{\sqrt{k!}}\frac{\left(\xi^{*}\alpha^{*}\left(t\right)\right)^{n}}{\sqrt{n!}}\left|k_{\mathrm{in}}\right\rangle\left\langle n_{\mathrm{in}}\right|.
\end{aligned}
$$

Putting everything together, we immediately see that (4.8) is verified for coherent states. Since coherent states constitute a basis of the Hilbert space (coherent states are a basis in the sense that there exists a completeness relation for such states (see app. E), rigorously, they form an overcomplete basis), we find that, by virtue of the linearity of the master equation, this proves that any state $\left|\psi\left(t\right)\right\rangle$ which can be cast in the form (see app. E)

$$
\left|\psi\left(t\right)\right\rangle=\frac{1}{\pi}\int\mathrm{d}\left(\mathfrak{Re}\xi\right)\int\mathrm{d}\left(\mathfrak{Im}\xi\right)c\left(\xi\right)\left|\xi_{\mathrm{in}}\left(t\right\rangle\right.
$$

is a solution of the Lindblad master equation provided that $c\left(\xi\right)$ does not depend on time.

5 Conclusions and prospects

We presented our investigations on various features of decaying quantum systems. Our toy-model for the Gamow potential allowed us to study the role of time in quantum mechanics, as we investigated why the standard "semiclassical" model of an α particle bouncing back and forth between the potential barriers, which can be said to classicaly treat the time variable, yields reasonable results (most notably, the Geiger-Nuttal law). We were able to refine the understanding of the Gamow model thanks to our numerical simulations which confirmed the results yielded by the complex pole formalism developed by Dürr *et al.*. We then turned gradually to cavity QED by first discussing open quantum systems for which we studied a simple model. Considering photons, *i.e* a linear dispersion relation, we derived an interesting result -exact in the case of photons- concerning the propagation of the "light wavefront" in the outside region. We found exponentially growing tails inside the light cone, a result similar to what is found in classical electrodynamics when one looks for the eigenmodes of an open system [35] by solving the source-free Maxwell's equations. It would be interesting to try and obtain -within a second quantisation framework- the precise spacetime distribution of the photons which escape the cavity (in our model, the potential barriers). This problem is related to the localisation of photons in quantum optics [38] and more generally to the issue of a realistic spacetime picture of particles in second quantisation [10]. Finally we used the Wigner-Weisskopf time-dependent perturbation theory to derive basic results about coherence and decoherence in a QED cavity.
Although our investigations throughout this work were carried out from a quantum point of view, many results among the ones we encoutered or derived carried similarities with non-quantum approaches to electrodynamics. Along with what we already mentioned, that is, the exponentially growing tails for "photonic" waves propagating outwards from an open quantum system and the quasi-classical status of coherent states for a QED cavity, let us note that a treatment in terms of Green's functions, exactly analogous to that found in [21] -and sketched in app. A- for quantum systems, is developed for classical electromagnetic systems in [37], where a solution to "renormalise" exponentially growing leaky eigenmodes is proposed. Building on these various remarks, we plan, among others, to estimate by classical methods (see sect. 4.2) the decay time of the cavity used by the QED team in Paris.
So far only a few experiments made it possible to observe non-exponential decay at long times. The short-time (Zeno) regime attracted much attention but the power-law behaviour which is

expected to occur at long times has seldom been investigated. We plan to study this regime by numerical methods, by choosing short-lived Gamow states as our initial state. We also plan to investigate quantum beats -that is, interferences- between modes, which would open the door to fundamental experiments concerning the status of time in quantum theory [23] [25].
Let us finally mention that we have shown [24] that coherent states are good candidates for pointer states in a general framework which goes beyond the non-Markovian regime considered here. It would be interesting to further study the general case, notably in light of the master equations.

A Derivation of the retarded Green's function for time-independent potentials: some key steps

In this appendix we give a certain number of intermediate results which pave the way to García-Calderón's final expression [21] for long-time deviations from exponential behaviour.

A.1 The outgoing Green's function and the retarded Green's function

What we want to do here is to solve the time-independent Schrödinger equation

$$-\frac{\hbar^2}{2m}\frac{\mathrm{d}^2\varphi}{\mathrm{d}x^2}+V(x)\,\varphi(x)=\frac{\hbar^2k^2}{2m}\varphi(x)\,. \tag{A.1}$$

Since we will eventually be interested in situations where a confined state decays outwards from the finite potential-region, we define the outgoing Green's function G^+ as a solution to

$$\frac{\hbar^2}{2m}\frac{\partial^2 G^+}{\partial x^2}\left(x,x';k\right)+\left(\frac{\hbar^2k^2}{2m}-V(x)\right)G^+\left(x,x';k\right)=\delta\left(x-x'\right) \tag{A.2}$$

with boundary conditions [21]

$$\begin{array}{rcl}\frac{\partial G^+}{\partial x}(-L,x';k) &=& -\mathrm{i}k\,G^+(-L,x';k)\,,\\ \frac{\partial G^+}{\partial x}(L,x';k) &=& \mathrm{i}k\,G^+(L,x';k)\,.\end{array} \tag{A.3}$$

We also define the retarded Green's function g as a solution to

$$\left(\mathrm{i}\hbar\frac{\partial}{\partial t}-H\right)g\left(x,x';t\right)=\mathrm{i}\hbar\,\delta\left(x-x'\right)\delta(t)\,. \tag{A.4}$$

We assert now that they are related by

$$g\left(x,x';t\right)=\frac{\mathrm{i}}{\pi}\int_{-\infty}^{+\infty}\mathrm{d}k\,\frac{\hbar^2k}{2m}G^+\left(x,x';k\right)\mathrm{e}^{-\mathrm{i}\frac{\hbar k^2}{2m}t}, \tag{A.5}$$

as can be readily checked. If we assume (A.5) to be true, then we have

$$\begin{aligned}\left(\mathrm{i}\hbar\frac{\partial}{\partial t}-H\right)g\left(x,x';t\right)&=\frac{\mathrm{i}}{\pi}\frac{\hbar^2}{2m}\int_{-\infty}^{+\infty}\mathrm{d}k\,k\left[\frac{\hbar^2}{2m}\frac{\partial^2}{\partial x^2}+\frac{\hbar^2k^2}{2m}-V(x)\right]G\left(x,x';k\right)\mathrm{e}^{-\mathrm{i}\frac{\hbar k^2}{2m}t}\\&=\frac{\mathrm{i}}{\pi}\frac{\hbar^2}{2m}\delta\left(x-x'\right)\int_{-\infty}^{+\infty}\mathrm{d}k\,k\,\mathrm{e}^{-\mathrm{i}\frac{\hbar k^2}{2m}t}\\&=\frac{\mathrm{i}}{2\pi}\frac{\hbar^2}{2m}\delta\left(x-x'\right)\int_{-\infty}^{+\infty}\mathrm{d}\alpha\,\mathrm{e}^{-\mathrm{i}\frac{\hbar\alpha}{2m}t}\\&=\mathrm{i}\hbar\,\delta\left(x-x'\right)\delta(t)\end{aligned}$$

and the proof is complete.

A.2 The outgoing Green's function and the Gamow functions

We now turn to the crucial relation between the outgoing Green's function and the Gamow functions. We define Gamow functions u_n as solutions to the Schrödinger equation for complex eigenvalues $\hbar^2\varkappa_n^2/(2m)\equiv\mathcal{E}_n-\mathrm{i}\Gamma_n/2$ and purely outgoing boundary conditions

$$\frac{\mathrm{d}u_n}{\mathrm{d}x}(-L)=-\mathrm{i}\varkappa_n u_n(-L)\,,\quad \frac{\mathrm{d}u_n}{\mathrm{d}x}(L)=\mathrm{i}\varkappa_n u_n(L)\,. \tag{A.6}$$

We now assert that the $\varkappa_n$ are the isolated poles of the outgoing Green's function. To our knowledge there is no general-case proof for this, but it can be shown at least for the square well potential [21]. This allows us to consider the residues ρ_n of the outgoing Green's function:

$$\rho_n\left(x,x'\right)=\lim_{k\to\varkappa_n}\left(k-\varkappa_n\right)G^+\left(x,x';k\right). \tag{A.7}$$

We can Laurent-expand the outgoing Green's function around its poles:

$$G^+\left(x,x';k\right)\underset{k\to\varkappa_n}{\sim}\frac{\rho_n\left(x,x'\right)}{k-\varkappa_n}+\chi\left(x,x';k\right), \tag{A.8}$$

and substituting this in (A.2) and (A.4), it is not too hard to see, taking the limit $k\to\varkappa_n$, that $\rho_n\left(\cdot,x'\right)$ satisfies the Schrödinger equation for eigenvalues $\varkappa_n$ and boundary conditions (A.6). Therefore, it is proportional to the Gamow functions u_n, and one can write

$$\rho_n\left(x,x'\right)=u_n\left(x\right)F\left(x'\right). \tag{A.9}$$

Thereafter, F can be computed using boundary conditions (A.6) and their equivalent in terms of ρ_n and χ, which yields

$$\rho_n\left(x,x'\right)=\frac{2m}{\hbar^2}\frac{u_n\left(x\right)u_n\left(x'\right)}{\varkappa_n}. \tag{A.10}$$

A.3 Long-time behaviour: the Moshinsky function

Using the tools of complex analysis, one can then show [21] that

$$G^+\left(x,x';k\right)=\frac{2m}{\hbar^2}\sum_n\frac{u_n\left(x\right)u_n\left(x'\right)}{2\varkappa_n\left(k-\varkappa_n\right)}, \tag{A.11}$$

which gives, using (A.4), the following expression for the retarded Green's function:

$$g\left(x,x';t\right)=\sum_n u_n\left(x\right)u_n\left(x'\right)M\left(\varkappa_n,t\right) \tag{A.12}$$

where M is the Moshinsky function defined by

$$M\left(\varkappa_n,t\right)=\frac{\mathrm{i}}{2\pi}\int_{-\infty}^{+\infty}\mathrm{d}k\frac{\mathrm{e}^{-\mathrm{i}\frac{\hbar^2k^2}{2m}t}}{k-\varkappa_n}. \tag{A.13}$$

The long-time behaviour of the wave function

$$\psi\left(x,t\right)\underset{t\to+\infty}{\sim}\sum_{n=1}^{+\infty}\left[c_nu_n\left(x\right)\mathrm{e}^{-\frac{\mathrm{i}}{\hbar}\mathcal{E}_nt}\mathrm{e}^{-\frac{1}{\hbar}\Gamma_nt}-\mathrm{i}\frac{\left(\frac{2m}{\hbar}\right)^{\frac{3}{2}}}{2\left(\mathrm{i}\pi\right)^{\frac{1}{2}}}\mathfrak{Im}\left(\frac{c_nu_n\left(x\right)}{\varkappa_n^3}\right)t^{-\frac{3}{2}}\right] \tag{A.14a}$$

where

$$c_n\equiv\int_{-L}^{L}\mathrm{d}x\,\psi\left(x,0\right)u_n\left(x\right) \tag{A.14b}$$

can then be retrieved using the asymptotic properties [8] of the Moshinsky function.

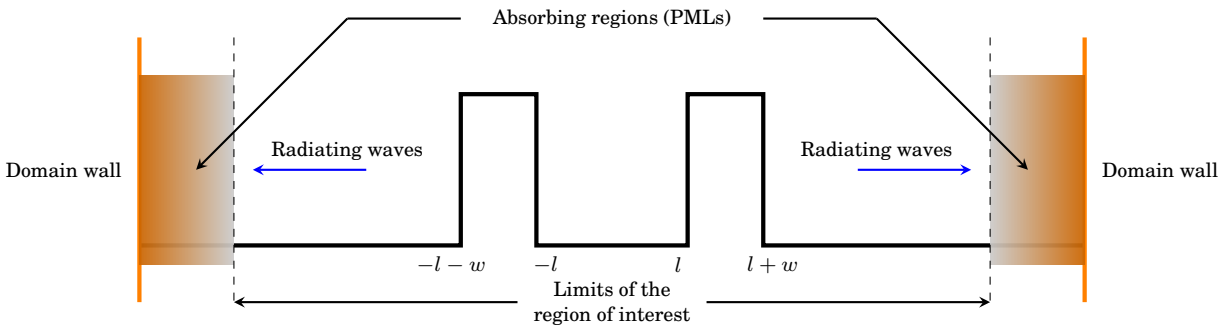

Figure B.1: Layout of the system within the PML framework. Near the domain walls, absorbing layers are artifically added into the program to avoid reflections. These regions are placed outside the "region of interest", which is not properly mathematically defined but rather well understood as the region where interesting phenomena take place.

B Taming the reflections: the perfectly matched layer (PML) method

B.1 Motivations and principles

One of the main problems when one wants to solve an equation numerically is that one is condemned to work in limited space. Since we are interested in decaying states, that is, states for which the wave function spreads with time, this is particularly bothersome: sooner or later, the wave function is bound to be reflected off the domain walls and propagate its way back into the zone of interest. This must absolutely be avoided since we want to know what happens in this zone. To tame these unphysical reflections, André Nicolet and Frédéric Zolla advised the author to use a well-known method in computational electromagnetism, the perfectly matched layer (PML) method.

This method is based on complex coordinate stretching in the absorbing zone [34]. Radiating waves are oscilating in x, but if we analytically continue the wave equation and thus its solutions in the complex plane, the radiating waves will be exponentially decaying in the regions where the coordinate stretching was performed, that is, in the absorbing layers. This coordinate stretching can be written in the following way:

$$x \to \tilde{x} = \left(1 + \mathrm{i}\eta\left(x\right)\right) x \tag{B.1}$$

where η is a real function of the real argument x, and vanishes everywhere except in the absorbing layers. We then have to solve the Schrödinger equation for the stretched variable $\tilde{x}$. The Laplacian operator takes the form

$$\begin{aligned}
-\frac{\hbar^2}{2m}\frac{\partial^2}{\partial x^2} &\to -\frac{\hbar^2}{2m}\left[\frac{1}{1+\mathrm{i}\eta\left(x\right)}\frac{\partial}{\partial x}\frac{1}{1+\mathrm{i}\eta\left(x\right)}\frac{\partial}{\partial x}\right] \\
&= -\frac{\hbar^2}{2m}\left[\frac{1}{\left(1+\mathrm{i}\eta\left(x\right)\right)^2}\left(-\frac{\mathrm{i}}{1+\mathrm{i}\eta\left(x\right)}\frac{\mathrm{d}\eta}{\mathrm{d}x}\frac{\partial}{\partial x}+\frac{\partial^2}{\partial x^2}\right)\right] \\
&= -\frac{\hbar^2}{2m}\frac{1}{\left(1+\eta^2\left(x\right)\right)^2}\left[\left(3-\eta^2\left(x\right)\right)\left(-\frac{\eta\left(x\right)}{\left(1+\eta^2\left(x\right)\right)}\frac{\mathrm{d}\eta}{\mathrm{d}x}\frac{\partial}{\partial x}\right)\right. \\
&\left.+\mathrm{i}\left(1-3\eta\left(x\right)\right)\left(-\frac{\eta\left(x\right)}{1+\eta^2\left(x\right)}\frac{\mathrm{d}\eta}{\mathrm{d}x}\frac{\partial}{\partial x}\right)+\left(1-\eta^2\left(x\right)-2\mathrm{i}\eta\left(x\right)\right)\frac{\partial^2}{\partial x^2}\right].
\end{aligned}$$

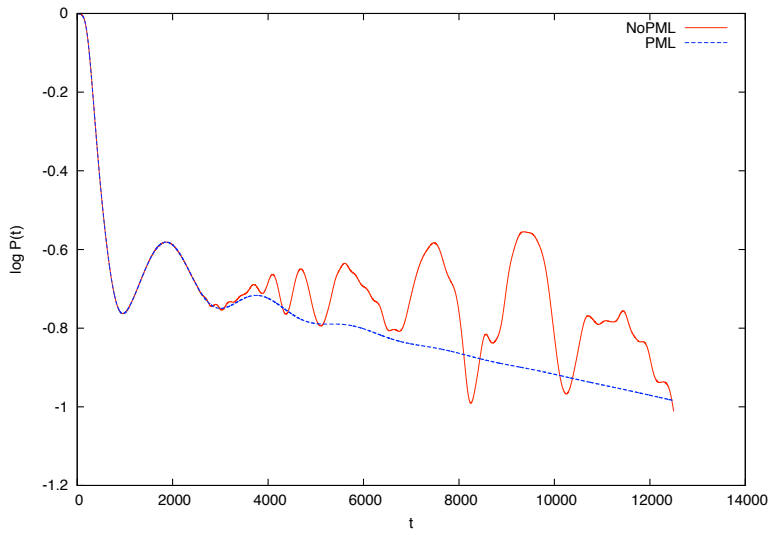

Figure B.2: Logarithm of the nonescape probability plotted against time without (red solid line) and with (blue dashed line) an absorbing layer. One can clearly see artifacts in the first case. These are due to reflections of the wave function off the domain limits. When one adds the absorbing layer, these reflections disappear.

We can then discretise the Schrödinger equation written with this new, analytically continued Laplacian operator, and solve it numerically with the same method as the one we outlined in sect. 2.3.

B.2 Results

To illustrate the efficiency of the PML method, we plotted in Figure B.2 the evolution of the natural logarithm of the nonescape probability

$$P_{\text{nonesc}}(t) \equiv \int_{-l}^{l} \mathrm{d}x \ |\psi(x,t)|^2 \tag{B.2}$$

with time. Figure B.2 displays the results obtained without any treatment of the reflections and the results yielded by the PML method. We clearly see artifacts: in the absence of absorbing layers there is what could be called a "revival" of the wave after $t \sim 2.5 \times 10^3$ time steps. This phenomenon, which is caused by the reflection of the wave function off the domain walls, completely disappears (or at least becomes so insignificant it is no longer visible) when we add the "shielding" absorbing layers.
To make sure these large oscillations are indeed due to reflections, we performed a series of tests, including increasing the phase velocity of the Schrödinger wave, and increasing the size of the computation domain so that the walls are farther away from the double barrier. All these tests conclusively showed that the wave function was indeed bouncing off the domain walls and reentering the well ($x \in [-l, l]$) region.

C The tetrachotomy method

In this appendix we present the elegantly named tetrachotomy method which underlies the algorithm we used to find the poles of the generalised eigenfunctions.

C.1 Motivations and principles

We see in app. D that the search for Gamow functions is reduced to the search for the poles of the generalised eigenfunctions. This is a common occurence. Hence we make use of the powerful properties of the functions of one complex variable to find the Gamow functions. We want to find

the poles of a meromorphic function f in $\mathbb{C}$, that is, a function for which there exists a sequence of points $\{\omega_i\}$ that has no limit points in $\mathbb{C}$ [6] such that:

- f is holomorphic in $\mathbb{C}\backslash\{\omega_i\}$.
- f has poles at points $\{\omega_i\}$.

We make use of the following result [6]: if f has a pole at ω_i then in a neighbourhood X_i of that point there exists a non-vanishing holomorphic function g and a unique positive integer n such that

$$f(z) = (z-\omega_i)^{-n} g(z). \tag{C.1}$$

Let us consider a Jordan loop Γ which belongs to the neighbourhood X_i of ω_i, that is, a Jordan loop which contains ω_i but no other pole of the function. We assume that the pole ω_i is simple and that g does not have a pole at $z=0$, so that we can rewrite it $g(z) = zh(z)$ with h holomorphic, and calculate the following integrals:

$$I_0 \equiv \frac{1}{2\mathrm{i}\pi}\int_\Gamma \mathrm{d}z \frac{f(z)}{z} = \frac{1}{2\mathrm{i}\pi}\int_\Gamma \mathrm{d}z \frac{h(z)}{z-\omega_i}, \tag{C.2a}$$

$$I_1 \equiv \frac{1}{2\mathrm{i}\pi}\int_\Gamma \mathrm{d}z f(z) = \frac{1}{2\mathrm{i}\pi}\int_\Gamma \mathrm{d}z\, z\frac{h(z)}{z-\omega_i}, \tag{C.2b}$$

$$I_2 \equiv \frac{1}{2\mathrm{i}\pi}\int_\Gamma \mathrm{d}z\, z f(z) = \frac{1}{2\mathrm{i}\pi}\int_\Gamma \mathrm{d}z\, z^2\frac{h(z)}{z-\omega_i}. \tag{C.2c}$$

Using the Cauchy residue theorem, it is straightforward to see that [9]

$$\omega_i = \frac{I_2}{I_1} = \frac{I_1}{I_0}. \tag{C.3}$$

Putting all this together for the situation schemed in Figure C.1, we conclude that for a rectangle Γ in the complex plane, if we perform the integral along Γ, three possibilities arise:

- $I_0 = I_1 = 0 \rightarrow$ there is no pole in the domain.
- $\frac{I_2}{I_1} = \frac{I_1}{I_0} \rightarrow$ there is a single pole in the domain.
- $\frac{I_2}{I_1} \neq \frac{I_1}{I_0} \rightarrow$ there are poles in the domain since the integrals are nonvanishing, but (C.1) is not valid, and hence there are several poles.

The principle of the tetrachotomy method is then, whenever the third situation arises, to divide the rectangle Γ into four equal rectangles Γ_i, and to repeat the process until the initial rectangle is divided into rectangles which all contain one pole at most. This is schemed in Figure C.1.

C.2 Numerical calculations and results

To compute the integral of a function q along a rectangle Γ, we write

$$\int_\Gamma \mathrm{d}z\, q(z) = \int_{\Gamma_{\mathrm{btm}}} \mathrm{d}z\, q(z) + \int_{\Gamma_{\mathrm{rgh}}} \mathrm{d}z\, q(z) + \int_{\Gamma_{\mathrm{top}}} \mathrm{d}z\, q(z) + \int_{\Gamma_{\mathrm{lft}}} \mathrm{d}z\, q(z). \tag{C.4}$$

The trajectories are then parametrised (see [9]). The final step is to make use of the so-called periodisation method. It is based on the fact that if the integrand is a function of class C^{2k} on the integration interval $[a,b]$ and its odd-order derivatives satisfy the condition

$$\forall p \in \{1,\cdots,k-1\}\ q^{(2p-1)}(a) = q^{(2p-1)}(b), \tag{C.5}$$

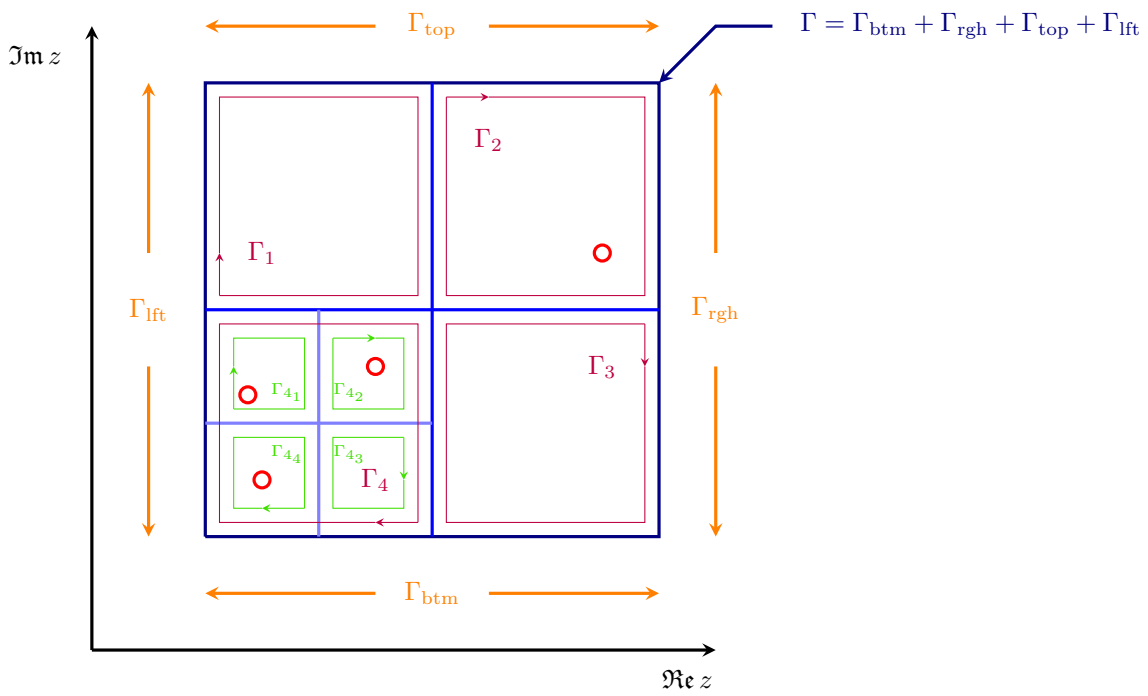

Figure C.1: The tetrachotomy algorithm performed on a rectangle in the complex plane. The poles are represented by red circles.

then the error yielded by the rectangle-method integration of $\int_a^b \mathrm{d}z\, q\,(z)$ behaves like $O\left(N^{-2k}\right)$ where N is the number of rectangles used to approximate the function. It is possible to find a change of variables (see [9] (sect. 3.4)) such that the parametrisation of the integrals yields an integrand that verifies condition (C.5). Hence the computation of the integrals is made fast and accurate.
The validity of the method can be highlighted in the following way: we simply build a meromorphic function by choosing poles and residues randomly, and we apply the algorithm on this function. We find (see Figure C.2) that the poles found by the program are extremely close to the ones we entered as input data.

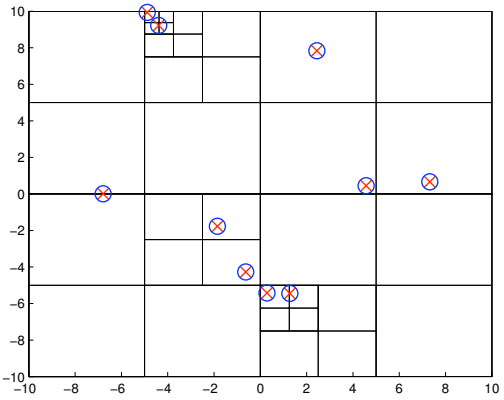

Figure C.2: The poles found using the tetrachotomy method for a test function (red crosses) plotted against the exact (simple) poles of the meromorphic test function (blue circles). Successive zooms show that the accuracy of the algorithm is excellent.

D Quantum scattering: complex poles and their eigenfunctions

Our discussion here follows [22]. We are considering the double barrier system (see sect. 2.3 and Figure 2.2), for which we want to write the normalised generalised eigenfunctions $u_\pm(k,\cdot)$ (there are two such functions because the Schrödinger equation is a second-order equation with respect to space coordinates). These functions form a basis on which to expand the solutions to the Schrödinger equation:

$$\varphi(x) = \int_0^{+\infty} \mathrm{d}k \, \left[\bar{\psi}_+(k)\, u_+(k,x) + \bar{\psi}_-(k)\, u_-(k,x)\right] \tag{D.1a}$$

$$\text{where} \quad \bar{\psi}_\pm(k) \equiv \int_{-\infty}^{+\infty} \mathrm{d}x\, \psi(x)\, u_\pm^*(k,x)\,. \tag{D.1b}$$

First, we look for the (nonnormalised) generalised eigenfunctions $f_\pm$. Since the potential has finite range, the ansatz is [22]

$$f_+(k,x) = \begin{cases} a_+(k)\,\mathrm{e}^{\mathrm{i}kx} \quad + \quad b_+(k)\,\mathrm{e}^{-\mathrm{i}kx} & \forall x \leq -l-w, \\ c_+(k)\,\mathrm{e}^{\mathrm{i}kx} & \forall x \geq l+w \end{cases} \tag{D.2a}$$

$$f_-(k,x) = \begin{cases} c_-(k)\,\mathrm{e}^{-\mathrm{i}kx} & \forall x \leq -l-w. \\ a_-(k)\,\mathrm{e}^{-\mathrm{i}kx} \quad + \quad b_-(k)\,\mathrm{e}^{\mathrm{i}kx} & \forall x \geq l+w, \end{cases} \tag{D.2b}$$

It is natural in order to normalise these eigenfunctions to take $a_\pm(k) = 1$, however it is not the choice that is made. Instead, we set $c_\pm(k) = 1$ and the normalisation, which has to ensure that

$$\delta(k-q) = \int \mathrm{d}x\, u_\pm(k,x)\, u_\pm^*(q,x)\,, \tag{D.3}$$

is yielded by the choice

$$u_\pm(k,x) = \frac{1}{\sqrt{2\pi}} \frac{f_\pm(k,x)}{a(k)} \tag{D.4}$$

where $a_+(k) = a_-(k) \equiv a(k)$ [22]. It is then clear that any root of a is a pole of $u_\pm(\cdot,x)$. As it turns out, the corresponding residue is precisely a Gamow function, *i.e.* a function that satisfies the Schrödinger equation for complex eigenvalue $\hbar^2k^2/(2m)$ as well as plane-wave-like conditions

$$\lim_{x\to\pm\infty} \left(G(x) - \mathrm{e}^{\pm\mathrm{i}kx}\right) = 0. \tag{D.5}$$

Note that the latter condition is slightly more restrictive than the one imposed in (A.6). The fact that the residue of the normalised generalised eigenfunction is a Gamow function can be showed by the following argument: defining the Wronskian $W(g,h)$ of two functions g and h to be

$$W(g,h)(x) = g(x)\,\frac{\mathrm{d}h}{\mathrm{d}x} - \frac{\mathrm{d}g}{\mathrm{d}x} h(x)\,, \tag{D.6}$$

one can readily show that $W_x(f_+,f_-)(k,x) = -2\mathrm{i}ka(k)$, so that when a vanishes (let us call ω such a point), so does the Wronskian, which, according to (D.6), means that $f_+(\omega,\cdot)$ and $f_-(\omega,\cdot)$ are proportional to each other. Taking a look at (D.2), this yields $b_\pm(\omega) = 1$. Putting all this together, we find that $f_\pm(\omega,\cdot)$ satisfies the plane-wave-like conditions (D.5). Since $f_\pm(\omega,\cdot)$ also solves the Schrödinger equation, it is clear that

$$f_\pm(\omega,x) = G(x)\,,$$

that is,

$$\operatorname*{Res}_{k=\omega} u_{\pm}(\cdot, x) = \eta\, G(x) \tag{D.7}$$

where η is simply a constant. This shows that the search for the Gamow functions' complex eigenenergies is simply a search for the poles of a. For our system, a can be calculated explicitly using continuity conditions for the wave function [22]: defining

$$q \equiv \sqrt{k^2 - \frac{2m}{\hbar} V_0}$$

and

$$A(k) = \cos(qw) - \frac{\mathrm{i}}{2}\left(\frac{k}{q} + \frac{q}{k}\right)\sin(qw), \tag{D.8}$$

it is given by

$$a(k) = a_1(k)\, a_2(k) \tag{D.9a}$$

$$\text{where} \quad a_{1/2}(k) = \mathrm{e}^{\mathrm{i}kw}\left(A(k) \mp \frac{\mathrm{i}}{2}\mathrm{e}^{2\mathrm{i}kl}\left(\frac{k}{q} - \frac{q}{k}\right)\sin(qw)\right). \tag{D.9b}$$

The search for a's poles allowed Dürr *et al.* [22] to retrieve the lifetime of radioactive uranium 234 with good accuracy: the experimental decay rate is $\Gamma_{\text{exp}} = 2.5872 \times 10^{-13}\,\text{s}^{-1}$, while the fitted theoretical value is $\Gamma_{\text{pole}} = 2.6722 \times 10^{-13}\,\text{s}^{-1}$. Using the same pole to compute the decay rate in the "semiclassical" approach yields a bouncing frequency of $f = 1.138 \times 10^{21}\,\text{s}^{-1}$ and a tunneling probability of $T = 2.751 \times 10^{-34}$, which means that $\Gamma_G = 3.130 \times 10^{-13}\,\text{s}^{-1}$, a fairly good approximation to the experimental value. For stability reasons, we were unable to produce numerical results for this system, since the algorithm's stability requirements forbade us to increase the numerical time step at will.

E Completeness relation for coherent states

Our goal here is to show that we can build a completeness relation for (damped) coherent states of the form (4.9) which we rewrite here:

$$|\xi_{\text{in}}(t)\rangle = \mathrm{e}^{-\frac{|\xi|^2}{2}|\alpha(t)|^2} \sum_{m=0}^{+\infty} \frac{(\xi\alpha(t))^m}{\sqrt{m!}}\, |m_{\text{in}}\rangle. \tag{E.1}$$

This completeness relation reads

$$\frac{1}{\pi}\int \mathrm{d}(\mathfrak{Re}\xi)\int \mathrm{d}(\mathfrak{Im}\xi)\, |\xi_{\text{in}}(t)\rangle\langle\xi_{\text{in}}(t)| = \hat{\mathbb{1}}, \tag{E.2}$$

as we prove now by switching to polar coordinates for ξ:

$$\begin{aligned}
\frac{1}{\pi}\int \mathrm{d}(\mathfrak{Re}\xi)\int \mathrm{d}(\mathfrak{Im}\xi)\, |\xi_{\text{in}}(t)\rangle\langle\xi_{\text{in}}(t)| &= \frac{1}{\pi}\int \mathrm{d}(\mathfrak{Re}\xi)\int \mathrm{d}(\mathfrak{Im}\xi)\, \mathrm{e}^{-|\xi|^2|\alpha(t)|^2} \sum_{m=0}^{+\infty}\sum_{k=0}^{+\infty} \frac{(\xi\alpha(t))^m}{\sqrt{m!}} \frac{(\xi^*\alpha^*(t))^k}{\sqrt{k!}}\, |m_{\text{in}}\rangle\langle k_{\text{in}}| \\
&= \frac{1}{\pi}\int_0^{+\infty} \mathrm{d}r\, r \int_0^{2\pi} \mathrm{d}\theta\, \mathrm{e}^{-r^2} \sum_{m=0}^{+\infty}\sum_{k=0}^{+\infty} r^{k+n} \frac{\mathrm{e}^{\mathrm{i}(m-k)\theta}}{\sqrt{m!}\sqrt{k!}}\, |, m_{\text{in}}\rangle\langle k_{\text{in}}| \\
&= \frac{1}{\pi}(2\pi)\,\delta_{nk} \int_0^{+\infty} \mathrm{d}r\, r \sum_{m=0}^{+\infty}\sum_{k=0}^{+\infty} r^{k+n} \frac{1}{\sqrt{m!}\sqrt{k!}}\, |m_{\text{in}}\rangle\langle k_{\text{in}}|
\end{aligned}$$

$$
\begin{aligned}
&= 2\int_0^{+\infty} \mathrm{d}r\, r \sum_{m=0}^{+\infty} r^{2m} \frac{1}{m!}\, |\, m_{\mathrm{in}}\rangle\langle m_{\mathrm{in}}\,| \\
&= \int_0^{+\infty} \mathrm{d}u\, \mathrm{e}^{-u} \sum_{m=0}^{+\infty} \frac{u^m}{m!}\, |\, m_{\mathrm{in}}\rangle\langle m_{\mathrm{in}}\,| \\
&= \sum_{m=0}^{+\infty} \frac{1}{m!} \Gamma\left(m+1\right)\, |\, m_{\mathrm{in}}\rangle\langle m_{\mathrm{in}}\,| \\
&= \sum_{m=0}^{+\infty} |\, m_{\mathrm{in}}\rangle\langle m_{\mathrm{in}}\,| \\
&= \hat{\mathbb{1}}
\end{aligned}
$$

and the proof is complete.

References

[1] A. Messiah, *Mécanique Quantique - Tome 1*, Dunod (1965).

[2] S. Haroche, J.-M. Raimond, *Exploring the Quantum - Atoms, Cavities and Photons*, Oxford University Press (2006).

[3] B.-G. Englert, *Lectures on Quantum Mechanics - Vol. 3: Perturbed Evolution*, World Scientific (2006).

[4] R.G. Newton, *Scattering Theory of Waves and Particles*, McGraw-Hill (1966).

[5] E.B. Davies, *Spectral Theory and Differential Operatos*, Cambridge University Press (1995).

[6] E.M. Stein, R. Shakarchi, *Complex Analysis*, Princeton University Press (2003).

[7] W. Appel, *Mathématiques pour la physique et les physiciens !*, H&K (2002).

[8] M. Abramowitz, I. A. Stegun, *Handbook of Mathematical Functions*, Dover Publications (1964).

[9] Y. Ould Agha, PhD Thesis: Transformations géométriques réelles et complexes : application à la recherche de modes à pertes dans des fibres optiques microstructurées, Université Paul Cézanne (2007).

[10] S. Colin, PhD Thesis: Bohm-Bell Beables for Quantum Field Theory, Vrije Universiteit Brussel (2005).

[11] R. Grummt, Diplomarbeit Thesis: On the Time-Dependent Analysis of Gamow Decay (2009).

[12] J.R. Nagel, *The One-Dimensional Finite-Difference Time-Domain Algorithm Applied to the Schrödinger Equation*, Notes available online.

[13] D. Ferreira, R. Pinto, *Gamow's Theory of Alpha Decay*, Notes available online.

[14] S. Perriès, *Physique Nucléaire - Ch. 6: Radioactivité α, β et γ*, Notes available online (lectures given in the fall semester of the 2010-2011 academic year to the first year students of the Master Sciences de la Matière at the École Normale Supérieure de Lyon).

[15] G. Gamow, "Zur Quantentheorie des Atomkernes", *Z. Phys.* **51**, 204 (1928).

[16] G. Gamow, "Zur Quantentheorie des radioaktiven Kerns", *Z. Phys.* **52**, 496 (1929).

[17] G. Gamow, "Zur Quantentheorie der Atomzertrümmerung", *Z. Phys.* **51**, 510 (1929).

[18] S. Haroche, D. Kleppner, "Cavity Quantum Electrodynamics", *Phys. Today* **42**, 24 (1989).

[19] S. Gleyzes, S. Kuhr, C. Guerlin, J. Bernu, S. Deléglise, U.B. Hoff, M. Brune, J.-M. Raimond, S. Haroche, "Quantum jumps of light recording the birth and death of a photon in a cavity", *Nature* **446**, 297 (2007).

[20] D. Bohm, "A Suggested Interpretation of the Quantum Theory in Terms of "Hidden" Variables I", *Phys. Rev.* **85**, 166 (1952).

[21] G. García-Calderón, "Transient effects in quantum decay", *AIP Conf. Proc.* **1334**, 84 (2011).

[22] D. Dürr, R. Grummt, M. Kolb, "On the time-dependent analysis of Gamow decay", *Eur. J. Phys.* **32**, 1311 (2011).

[23] C. Champenois, T. Durt, "Quest for the Time Operator with a Single Trapped Ion", *Int. J. Quant. Inf.* **9**, 189 (2011).

[24] T. Durt, V. Debierre, "Coherent states and the classical-quantum limit considered from the point of view of entanglement", submitted.

[25] M. Courbage, T. Durt, S.M. Saberi Fathi, "Quantum-mechanical decay laws in the neutral kaons", *J. Phys. A.* **40**, 2773 (2007).

[26] M. Courbage, T. Durt, S.M. Saberi Fathi, "Two-level Friedrichs model and kaonic phenomenology", *Phys. Lett. A* **362**, 100 (2007).

[27] W.H. Zurek, "Pointer basis of quantum apparatus: Into what mixture does the wave packet collapse?", *Phys. Rev. D* **24**, 1516 (1981).

[28] W.H. Zurek, "Environment-induced superselection rules", *Phys. Rev. D* **26**, 1862 (1982).

[29] W.H. Zurek, "Decoherence and the Transition from Quantum to Classical", *Phys. Today* **44** (10), 36 (1991).

[30] W.H. Zurek, "Quantum Darwinism", *Nat. Phys.* **5**, 181 (2009).

[31] J.P. Paz and W.H. Zurek, "Quantum Limit of Decoherence: Environment Induced Superselection of Energy Eigenstates", *Phys. Rev. Lett.* **82**, 5181 (1999).

[32] M. Schlosshauer, "Decoherence, the measurement problem, and interpretations of quantum mechanics", *Rev. Mod. Phys.* **76**, 1267 (2004) .

[33] E. Schrödinger, "Der stetige Übergang von der Mikro- zur Makromechanik", *Naturwissenschaften* **14**, 664 (1926).

[34] Y. Ould Agha, F. Zolla, A. Nicolet, S. Guenneau, "On the use of the PML for the computation of leaky modes: an application to gradient index MOF", *COMPEL* **27**, 95 (2008).

[35] B. Vial, A. Nicolet, F. Zolla, G. Demésy, M. Commandré, S. Tisserand, "Transformation Optics PML and quasi-mode analysis: application to diffraction gratings", submitted.

[36] E. Brainis, P. Emplit, "Wave function formalism in quantum optics and generalized Huygens-Fresnel principle for N photon-states: derivation and applications, *Proc. SPIE* **72727**, 772770 (2010).

[37] E.A. Muljarov, W. Langebin, R. Zimmerman, "Brillouin-Wigner perturbation theory in open electromagnetic systems", *Europhys. Lett.* **92**, 50010 (2010).

[38] T. Häyrynen, J. Oksanen, J. Tulkki, "Quantum aspects of optical energy transfer in cavities and layered media", *Proc. SPIE* **8440**, 844007 (2012).